



Doc:	DEL-27 Validation Report		
Date:	06.05.2014		
Issue:	1	Revision:	0
			Page 1



**DUE Coastcolour  
Validation Report  
Deliverable DEL-27**

Version 1.0

06. May 2014



<b>Doc:</b>	DEL-27 Validation Report		
<b>Date:</b>	06.05.2014		
<b>Issue:</b>	1	<b>Revision:</b>	0
			<b>Page 2</b>

	Doc:	DEL-27 Validation Report		
	Date:	06.05.2014		
	Issue:	1	Revision:	0

## The Coastcolour Team



**BROCKMANN  
CONSULT**

With



## And the Consultant Team

- Dr. Yu-Hwan Ahn (KORDI)
- Dr. Jim Gower (DFO)
- Dr. Mark Dowell (JRC)
- Dr. Stewart Bernard (CSIR)
- Dr. Zhongping Lee (U. Mississippi)
- Dr. Bryan Franz (NASA)
- Dr. Thomas Schroeder and Dr. Arnold Dekker (CSIRO)



<b>Doc:</b>	DEL-27 Validation Report		
<b>Date:</b>	06.05.2014		
<b>Issue:</b>	1	<b>Revision:</b>	0
			<b>Page 4</b>

	<b>Doc:</b>	DEL-27 Validation Report		
	<b>Date:</b>	06.05.2014		
	<b>Issue:</b>	1	<b>Revision:</b>	0

## Revision History

Version	Date	Change	Author
1	06.05.14	initial version	A. Ruescas, C. Brockmann, K. Stelzer, G. Tilstone, J. Beltran



<b>Doc:</b>	DEL-27 Validation Report		
<b>Date:</b>	06.05.2014		
<b>Issue:</b>	1	<b>Revision:</b>	0
			<b>Page 6</b>

	<b>Doc:</b>	DEL-27 Validation Report		
	<b>Date:</b>	06.05.2014		
	<b>Issue:</b>	1	<b>Revision:</b>	0

## Contents

1	SCOPE OF THIS DOCUMENT .....	9
2	INTRODUCTION .....	9
3	COASTCOLOUR PRODUCTS .....	10
3.1	CC L1P .....	10
3.2	CC L2R .....	10
3.3	CC L2W .....	10
4	METHODS .....	11
4.1	Reference Data .....	11
4.1.1	PixBox .....	11
4.1.2	Ocean Colour data .....	12
4.1.3	Match-up definition .....	13
4.2	Validation methods .....	13
4.2.1	PixBox evaluation and confusion matrix .....	13
4.2.2	Linear Regression .....	15
4.2.3	Statistical Measures .....	16
4.2.4	Profile Plots and Transect Analysis .....	16
4.2.5	Time Series Analysis .....	17
5	RESULTS .....	17
5.1	L1P products .....	17
5.1.1	Land - Water masking .....	17
5.1.2	Cloud masking .....	18
5.2	L2R products .....	21
5.2.1	Match-up analysis .....	21
5.2.2	Performance for very high turbid waters .....	23
5.2.3	Glint correction .....	26
5.3	L2W products .....	27
5.4	Case studies .....	35
5.4.1	North Sea and Western English Channel .....	35
5.4.2	North Sea time series .....	36
5.4.3	Baltic Sea (Sweden) .....	40
6	CONCLUSION .....	43
7	REFERENCES .....	44

	<b>Doc:</b>	DEL-27 Validation Report		
	<b>Date:</b>	06.05.2014		
	<b>Issue:</b>	1	<b>Revision:</b>	0

8	ACKNOWLEDGEMENTS .....	44
9	ANNEX 1: VALIDATION REPORT FOR COASTCOLOUR MERIS LEVEL2 PRODUCTS IN CASE 2 WATERS OF THE NORTH SEA AND WESTERN ENGLISH CHANNEL.....	44

	Doc:	DEL-27 Validation Report		
	Date:	06.05.2014		
	Issue:	1	Revision:	0

## 1 SCOPE OF THIS DOCUMENT

This document provides the validation information for the Version 2 of the CoastColour processing and products. It aims at qualifying and quantifying the accuracy of the MERIS coastal water products generated with the version of the CoastColour processing chain. The corresponding products can be generated using the CoastColour On Demand Processing facility (see [www.coastcolour.org](http://www.coastcolour.org)), or using the publicly available CoastColour BEAM plug-ins (also available from the plug-in manager of BEAM, <http://www.brockmann-consult.de/cms/web/beam/>).

This document is structured as follows:

- Chapter 2 provides a brief introduction and describes the changes from CoastColour Version 1 to Version 2 processing
- Chapter 3 summarizes the CoastColour products available to users
- Chapter 4 describes the data and methods used in this validation report
- Chapter 5 describes the results of the validation
- Chapter 6 concludes on the results

## 2 INTRODUCTION

The European Space Agency has launched the CoastColour project to fully exploit the potential of the MERIS instrument for remote sensing of the coastal zone. The product requirements have been derived from a user consultation process. CoastColour is developing, demonstrating, validating and intercomparing different Case 2 algorithms over a global range of coastal water types, identifying best practices, and promoting discussion of the results in an open, public form. In May 2013 the CoastColour Version 1 dataset was released to the public. The MERIS Full Resolution Data of 27 globally distributed sites and covering the time range from 2005 - 2012 were processed with the first version of the processing algorithms. A resulting dataset of ~100TB of data was put online for download to the users.

Validation and assessment of Version 1 products have demonstrated the excellent quality of the CoastColour water leaving reflectances, and of IOPs and water constituents for turbid and extreme turbid waters. However, shortcomings were found specifically for the chlorophyll product in clear and slightly turbid waters (up to 5-10mg/m<sup>3</sup> TSM). Consequently, algorithm improvements were developed addressing this problem, which lead to the new version of the CoastColour algorithms. Additionally more MERIS FR data should be made available to the user community for a Version 2 processing.

Version 2 processing now includes:

- Full Mission archive (global, 2002 - 2012) of MERIS L1b FRS as well as RR products with harmonized calibration and consistent with the 3rd MERIS Reduced Resolution (RR) reprocessing are used as input data.
- L1P processing with improved geolocation, additional radiometric improvements (coherent noise equalisation, Smile correction) and pixel classification (cloud screening, improved land-sea mask, other pixel attributes). Performing adjacency correction is optionally possible.
- L2R processing applying a neural network based atmospheric correction, which is applicable for a large range of water type, from clear to extreme scattering waters.
- L2W processing providing water properties, such as inherent optical properties, chlorophyll and suspended matter concentration, diffuse attenuation coefficient K<sub>d</sub> and Secchi Disk Depth. In V2 processing an improved algorithm is applied for the chlorophyll-a retrieval using a blending of clear water OC4 algorithm and a neural network for turbid waters.

### 3 CoastColour Products

This chapter provides a brief summary of the standard CoastColour products v2.

#### 3.1 CC L1P

The Level 1P product is a refined top of atmosphere radiance product compared with the standard Level 1b product. It provides improved geolocation, equalisation to reduce coherent noise, smile correction, pixel characterization information (cloud, snow, etc.), a precise coastline and a reformatting into NetCDF following Climate Forecast (CF) conventions. NetCDF format is the CoastColour default; other output formats are GeoTIFF and BEAM-DIMAP.

Dataset	Band Name	Contents
L1P	radiance_i	Pre-processed MERIS TOA radiances.
	lat, lon, altitude	Ortho-corrected geo-coding.
	l1_flags	Copy of input Level 1 flags
	l1p_flags	Additional pixel classification information: - land, coastline from improved geocoding and SRTM land-water map - cloud flags - snow/ice flag - water/land mixed pixel - glint risk

#### 3.2 CC L2R

The Level L2R product is the result of the atmospheric correction. It contains water leaving reflectance, normalised water leaving reflectance and different information about atmospheric properties. It also contains an ortho-corrected geo-coding and different flags characterizing pixels.

L2R	reflec, norm_reflec atm_tau_550, ang_443_865	Contains water leaving reflectances, normalised water leaving reflectances, aerosol optical depth and angstrom exponent. Optionally the user can add other variables (using the Calvalus On-Demand processing or the BEAM CoastColour processor)
	lat, lon, altitude	Ortho-corrected geo-coding.
	l1_flags, l1p_flags	Copy of flags provided in the L1P product
	l2r_flags	Flags providing additional information on the atmospheric processing

#### 3.3 CC L2W

The L2W product provides information about water properties such as IOPs, concentrations and other variables. It also contains an ortho-corrected geo-coding and different flags characterizing pixels.

L2W	iop_a_total, iop_a_ys_443, iop_a_pig_443, iop_bb_spm_443, iop_a_det_443, iop_b_tsm_443, iop_b_whit_443, iop_a_dg_443, iop_quality	Inherent optical water properties calculated by a neural network
	qaa_iop_a_total_443, qaa_iop_a_ys_443, qaa_iop_a_pig_443, qaa_iop_bb_spm_443	Inherent optical water properties calculated by the QAA algorithm
	conc_tsm, conc_chl_nn, conc_chl_oc4, conc_chl_merged, conc_chl_weight	Concentrations of water constituents. The chlorophyll concentration is calculated twice for each pixel: with a neural network which performs best for high turbid waters (conc_chl_nn), and the OC4 algorithm (conc_chl_oc4). A blending between the two variables is done based on the tsm concentration. The weight provides the relative portion of the chl_nn.
	kd, z90_max, turbidity	Other water properties (spectral Kd and Kd_min, Z90_max, turbidity_index)
	- Not in CoastColour on demand processing but available offline as BEAM processor -	Fluorescence line height, Maximum chlorophyll index
	kd, z90_max, turbidity	Other water properties (spectral Kd and Kd_min, Z90_max, turbidity_index)
	lat, lon, altitude	Ortho-corrected geo-coding
	l1_flags, l1p_flags	Copy of flags provided in the L1P product
	l2r_flags	Copy of flags provided in the L2R product
	l2w_flags	Water constituents and IOPs retrieval quality flags

## 4 METHODS

### 4.1 Reference Data

#### 4.1.1 PixBox

Validation of pixel classification by comparison with reference data is a difficult task. In-situ observations that correspond with pixel classes such as cloud or turbid water are generally not possible. We use as reference data manually classified pixels. The method has been developed over several years and is known as PixBox dataset<sup>1</sup>.

For CoastColour an expert has collected 25.500 MERIS FR pixels over coastal areas, globally distributed. The spatial distribution of the data is shown in Figure 1. The data were taken from a random sample of MERIS products from the whole archive, i.e. between 2002 and 2012. The data were collected to have an even distribution between all seasons. The distribution among the different cloud/clear sky conditions is:

<sup>1</sup> Brockmann et al, 2012, IdePix Approach and validation using PixBox. Sentinel 2 Preparatory Symposium, [http://www.congrexprojects.com/docs/12c04\\_docs2/poster2\\_39\\_brockmann.pdf?sfvrsn=2](http://www.congrexprojects.com/docs/12c04_docs2/poster2_39_brockmann.pdf?sfvrsn=2)

totally cloudy	7691 pixels	30%
clear sky over water	7577 pixels	30%
non clear sky over water (=turbid atmosphere, semi-transparent cloud)	5127 pixels	20%
spatially mixed cloud/water	5102 pixels	20%

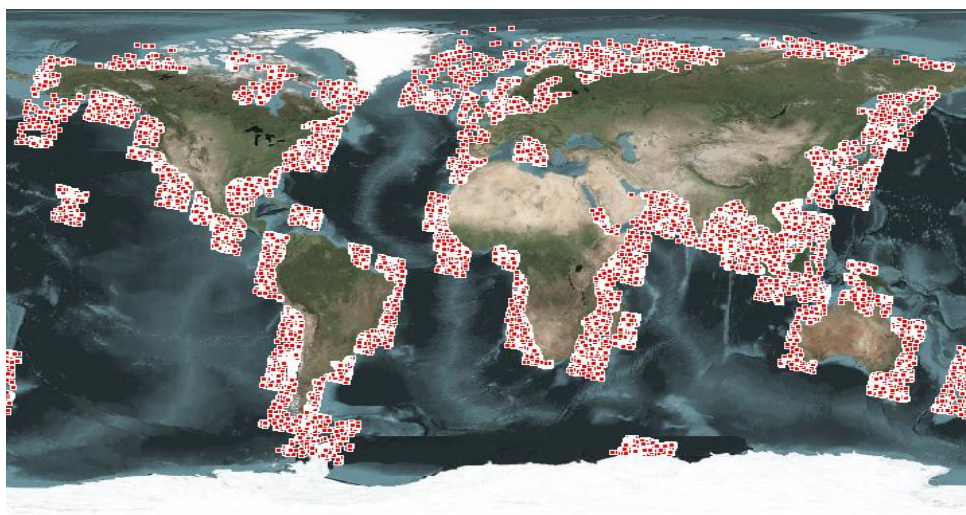


Figure 1: Spatial distribution of 18.500 MERIS FR samples collected for validation of the L1P pixel classes.

#### 4.1.2 Ocean Colour data

In order to enable a sound statistical comparison a set of marine geophysical reference data for the different coastal-sea areas has been collected within the CoastColour in-situ database as well as by means of the Mermaid matchup database. The CoastColour in-situ database is described in the DUE CoastColour in-situ database document<sup>2</sup>. A total of 1,280,203 records were assembled from various champion users, including ferry box data which contributed most of the records due to its continuous data collection system. Most of the data in the CoastColour in-situ database are in-water concentrations, primarily chlorophyll-a concentration and suspended matter concentrations.

The MERMAID dataset is quite complementary as its origin was marine reflectances for validation of the standard MERIS atmospheric correction. Meanwhile MERMAID includes insitu measurements of both, marine reflectances as well as in-water concentrations. It consists of datasets from PIs using a variety of measurement systems and following different measurement protocols, including SeaPRISM CIMEL, TACCS, fixed buoys, handheld radiometers and profiling instruments. Two comprehensive documents overviewing MERMAID and describing these in-situ protocols are available: the Apparent Optical Properties protocols<sup>3</sup>, and the Inherent Optical Properties and in-water constituents protocols<sup>4</sup>.

MERMAID contains chlorophyll from HPLC pigment analysis, using spectrophotometric procedures and fluorometric procedures. It also includes total suspended matter (TSM) and different types of absorption (detrital, particulate, algal pigment, yellow substance and total), as well as backscatter

<sup>2</sup> [http://www.coastcolour.org/documents/TN\\_CC\\_in-situ\\_database\\_v1.4.pdf](http://www.coastcolour.org/documents/TN_CC_in-situ_database_v1.4.pdf)

<sup>3</sup> [http://hermes.acri.fr/mermaid/dataproto/CO-SCI-ARG-TN-0008\\_In-situ\\_Measurement\\_Protocols-AOPs\\_Issue2\\_Mar2013.pdf](http://hermes.acri.fr/mermaid/dataproto/CO-SCI-ARG-TN-0008_In-situ_Measurement_Protocols-AOPs_Issue2_Mar2013.pdf)

<sup>4</sup> [http://hermes.acri.fr/mermaid/dataproto/CO-SCI-ARG-TN-0008\\_In-situ\\_Measurement\\_Protocols-IOPs-Constituents\\_Issue1\\_Mar2013.pdf](http://hermes.acri.fr/mermaid/dataproto/CO-SCI-ARG-TN-0008_In-situ_Measurement_Protocols-IOPs-Constituents_Issue1_Mar2013.pdf)

	Doc:	DEL-27 Validation Report		
	Date:	06.05.2014		
	Issue:	1	Revision:	0

(bb), diffuse attenuation ( $K_d$ ), normalised water reflectance ( $\rho_{wn}$ ) and different auxiliary parameters (aerosol optical thickness, distance to coast, azimuth angle, etc.).

The Mermaid database provides text files of in situ data, matched with concurrent and comparable MERIS L2 products (including flags, auxiliary information and the intermediate outputs of the processing). The extraction interface allows the users to select matchups according to their own requirements for site, parameters, flags and statistical screening, and produces validation statistics and plots. The Mermaid database is used to extract all possible in situ measurements in the different CoastColour sites. The matchup definition is explained in the next section. We needed to define the matchups twice: 1) to extract the measurements from Mermaid, 2) to find matchups on the CoastColour processing in Calvalus using the Mermaid in situ data as reference.

A second data set has been used for producing time series comparisons between in situ measurements and CoastColour chlorophyll concentration. The measurements have been provided by BSH (Federal Maritime and Hydrographic Agency) which they performed within their monitoring activities. Chlorophyll has been derived by HPLC analyses, we show here results from the cruises performed in 2010 in the North Sea.

#### 4.1.3 Match-up definition

Based on previous studies (GMES-MC-2-C6, MVT) it was determined that the shorter time difference between in situ and EO measures, the better, with a limit of  $\pm 3$  hours. A macro-pixel size of  $3 \times 3$  pixels is selected with the confidence of keeping at least three or more pixels for calculating the average of the measurement. The maximum scattering angle was taken as default ( $180^\circ$ ), and the same with the maximum sun zenith angle ( $60^\circ$ ) and maximum wind speed (9 m/s). All possible in situ data for all sites in the Mermaid dataset were extracted, being the data of the Mermaid file extraction from September 2012. This file has been kept as reference to be able to compare the different iterations of the neural net along these last two years. Previous comparisons with other versions of the NN have been done, and it is worthy to use the same dataset to better identify changes.

Due to the fact that temporal variability in chlorophyll concentration decreases with increasing distance from coast, and that the criteria “at least 6 valid pixels” that was used in the Marcoast validation exercise can partly counteract the proximity to the coast, we relaxed the requirements and accepted that at least one pixel within the macro-pixel had to be valid.

The validity of the pixels within the macropixels was based on the use of the land, cloud and PCD flags to mask the invalid ones, changing PCDs depending on the parameter to be used:  $\rho_{wn}$ , chlorophyll, TSM or absorption values. After the averages of the different parameters have been done, the output file is used as input in the Calvalus system to extract the level 2 radiance reflectance quality parameter from the CoastColour neural net.

For the validation of the in water parameters (CHL, TSM and YS), a new extraction of the Mermaid database was used to be able to have the maximum number of matchups possible. The latest Mermaid file was downloaded using the criteria explained before.

The matchup analysis in Calvalus also requires a macro pixels size definition, a maximum time difference and a good pixel expression. The values were set to  $1 \times 1$  pixel, with a maximum time difference of  $\pm 3$  hours and a good-pixel expression that excluded pixels flagged as L2R or L2W invalid. In Table 2 and Table 3, the total number of matchups left in each case is indicated in column “Number of samples”.

## 4.2 Validation methods

### 4.2.1 PixBox evaluation and confusion matrix

Beside a visual inspection of sample products a quantitative evaluation of the performance of the cloud screening (or the pixel classification in general) is performed using the PixBox database which contains 25,497 samples of manually classified MERIS FR pixels (see section 4.1.1). This database

actually contains only the attributes assigned by the expert, and the reference to the MERIS FR source product and pixel number. The source product is processed to L1P. A comparison process is extracting the attributes of the pixel in the source product and constructing a record in a table, which merges the manual classification and the L1P attributes. The procedure is depicted in Figure 2. Please note that this figure uses “IdePix” to indicate the processing to L1P as this is the name of the pixel classification process within the L1P processor.

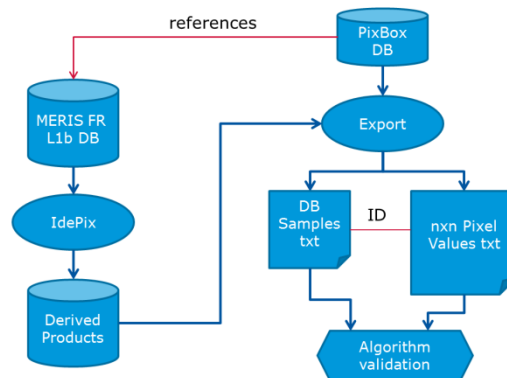


**Figure 2: Method of validation of the pixel identifications**

The evaluation is done by means of a confusion matrix, whose principle is presented in Figure 3 Fehler! Verweisquelle konnte nicht gefunden werden.. Columns contain the “truth”, which is - in the case of the PixBox dataset - the number of pixel per class as assigned by the expert. Rows contain the corresponding results of the algorithm, in this case the L1P algorithm. Ideally, only the main diagonal should be populated. The producer’s accuracy measures how well pixels, which belong in reality to a certain class, are correctly identified by the algorithm. As an example, if Class 1 would be “cloud” and Class 2 would be clear water, the producer’s accuracy for the class 1 cloud would be the percentage of classifying a cloud as cloud and not as clear water. On the contrary, the user’s accuracy represents the reliability of a detected class. In the same example as before, the user’s accuracy of the class cloud would indicate the percentage (or probability) that a pixel classified as cloud is really a cloudy pixel.

There are two key requirements for cloud screening, which are generally in competition:

- The class “clear water” should contain a minimum number of cloud pixels, i.e. the producer’s accuracy of the class “cloud” should be very high;
- The number of correctly classified clear sky water pixel should be high, i.e. the producer’s accuracy and the user’s accuracy of the class “clear sky water” should be high.

An algorithm which classifies every pixel as a cloud would have a very high producer’s accuracy for the cloud class (all cloud pixels would be detected as such), but the producer’s and user’s accuracy of the clear sky water class would be zero or undefined.

		Conditions				Users Accuracy
		Class I	Class II	...	Class N	
Algorithm	Class I	$a_{11}$	$a_{12}$	...	$a_{1n}$	$\frac{a_{11}}{\sum_{i=1}^n a_{1i}}$
	Class II	$a_{21}$	$a_{22}$	...	$a_{2n}$	$\frac{a_{22}}{\sum_{i=1}^n a_{2i}}$
	⋮	⋮	⋮	⋮	⋮	...
	Class N	$a_{n1}$	$a_{n2}$	...	$a_{nn}$	$\frac{a_{nn}}{\sum_{i=1}^n a_{ni}}$
Producers Accuracy		$\frac{a_{11}}{\sum_{i=1}^n a_{i1}}$	$\frac{a_{22}}{\sum_{i=1}^n a_{i2}}$	...	$\frac{a_{nn}}{\sum_{i=1}^n a_{in}}$	<b>Overall Accuracy</b> $\sum_{i=1}^n a_{ii}$ <i>for <math>\sum_{i=1}^n \sum_{j=1}^n a_{ij} = 1</math></i>

**Figure 3: Principle of the confusion matrix**

#### 4.2.2 Linear Regression

The method consists on study the correlation between two parameters by means of the regression analysis. The regression analysis is used to specify and test the functional relationship between variables. The linear regression analysis assumes that a linear regression exists between the dependent variable ( $y$ ) and the independent variable ( $x$ ). It proceeds by fitting a straight line to the set of observed data, and is the concerned with the interpretation and analysis of the effects of the  $x$  variables on  $y$ , and with the nature of the fit.

When there is just one independent variable, it is useful to fit a straight line through the set of data points. The equation of this line is:

$$\hat{y} = a + bx$$

where  $\hat{y}$  is the predicted value of the dependent variable,  $x$  is the observed value of the independent variable,  $a$  is the intercept (or point where the line intersects the vertical axis), and  $b$  is the slope of the line. The quantities  $a$  and  $b$  are parameters describing the line. This is the typical case of simple regression or bivariate regression. The slope of the line,  $b$ , may be interpreted as the change in the dependent variable expected from a unit change in the independent variable. The intercept  $a$  is the predicted value of the dependent variable when the independent variable is set equal to zero. In studying the linear relationship between variables, each observation of the dependent variable,  $y$ , may be expressed as the sum of a predicted value and a residual term:

$$y = a + bx + e = \hat{y} + e$$

where  $\hat{y} = a + bx$  is the predicted value, and  $e$  is termed the residual. The value  $\hat{y}$  represents the value of the dependent variable predicted by the regression line. The residual is equal to the difference between observed and predicted values:

$$e = y - \hat{y}$$

	<b>Doc:</b> DEL-27 Validation Report			
	<b>Date:</b> 06.05.2014			
	<b>Issue:</b> 1	<b>Revision:</b> 0	<b>Page 16</b>	

In regression analysis, the aim is to find the slope and intercept of the best fitting line that runs through the observed set of data points. The sum of the squared vertical distance from the observed points to the line is minimized in linear regression. This vertical distance is identical to the value of the residual. Thus regression analysis minimizes the sum of squared residuals:

$$\min_{a,b} \sum_{i=1}^n (y_i - a - bx_i)^2$$

The variability observed in  $y$  must be decomposed in one explained part and one part that remains unexplained:

$$\sum_{i=1}^n (y_i - \bar{y})^2 = \sum_{i=1}^n (\hat{y}_i - \bar{y})^2 + \sum_{i=1}^n (y_i - \hat{y}_i)^2$$

The proportion of the total variability in  $y$  explained by the regression is called the coefficient of determination, and it is equal to the square of the correlation coefficient:

$$r^2 = \frac{\sum_{i=1}^n (\hat{y}_i - \bar{y})^2}{\sum_{i=1}^n (y_i - \bar{y})^2}$$

The value  $r^2$  varies for 0 to 1, from non variability explained to all of residuals are zero and regression line fits perfectly through all the observed points.

#### 4.2.3 Statistical Measures

RMSE is a frequently used measure of the differences between values predicted by a model or an estimator and the values actually observed. The RMSE represents the sample standard deviation of the differences between predicted values and observed values. These individual differences are called residuals when the calculations are performed over the data sample that was used for estimation, and are called *prediction errors* when computed out-of-sample. The RMSE serves to aggregate the magnitudes of the errors in predictions for various times into a single measure of predictive power. RMSE is a good measure of accuracy to compare forecasting errors of different models for a particular variable.

$$MSE = \frac{1}{n} \sum_{i=1}^n (\hat{y}_i - y_i)^2$$

$$RMSE = \sqrt{MSE}$$

#### 4.2.4 Profile Plots and Transect Analysis

Profile plots provide another useful graphical summary of the data. They show the variation in each of the variables, by plotting the value of each of the variables for each of the samples. In the present report, the profile plot that is used the most is the spectral profile, which plots the spectrum

	Doc:	DEL-27 Validation Report		
	Date:	06.05.2014		
	Issue:	1	Revision:	0

of all bands for the selected pixel. Header information can be used to scale the plot or this is inserted manually for making the plots intercomparable.

A transect on an image can also be plotted using the profile plot. All pixels of an image that lie beneath the transect are plotted against a spectrum value or a parameter's value.

#### 4.2.5 Time Series Analysis

Time series refers to the association of variables with dates or periods of time. The representation of the behaviour of a parameter during a determined period assumes two different types of data: the observation itself, and the date at which it took place.

Time series analysis comprises methods for analyzing time series data in order to extract meaningful statistics and other characteristics of the data. The clearest way to examine a regular time series is with a line chart, which is, plotting the variable in line with the time of occurrence (**Fehler! Verweisquelle konnte nicht gefunden werden.**). Other techniques include the autocorrelation analysis to examine serial dependence (like regression analysis) and the spectral analysis or frequency domain analysis to examine cyclic behaviour which need not be related to seasonality.

Time series plots are important for users for the interpretation of the seasonal development of algal blooms, for instance. Indicators like the start date of a bloom, the duration or the intensity / spatial area are additional information that can be extracted from the data.

## 5 Results

### 5.1 L1P products

#### 5.1.1 Land - Water masking

The performance of the land-water masking is demonstrated visually at the example below. The coastline is clearly visible in the RGB (top), including the separation of the land area from the coastal sea and the lagoons in the upper right corner. The centre image shows in green overlay the standard MERIS L1b land flag, which is systematically shifted by ~2 pixels to the south, but the misplacement can reach up to 5 pixels. The lagoons are only half of their true size, and some lagoon pixels flagged as water are actually located on land. The CoastColour L1P land-water classification is shown in the bottom image as brown overlay. The land sea border matches exactly the radiometry and the lagoons keep their true size. No land pixels are erroneously flagged as water.

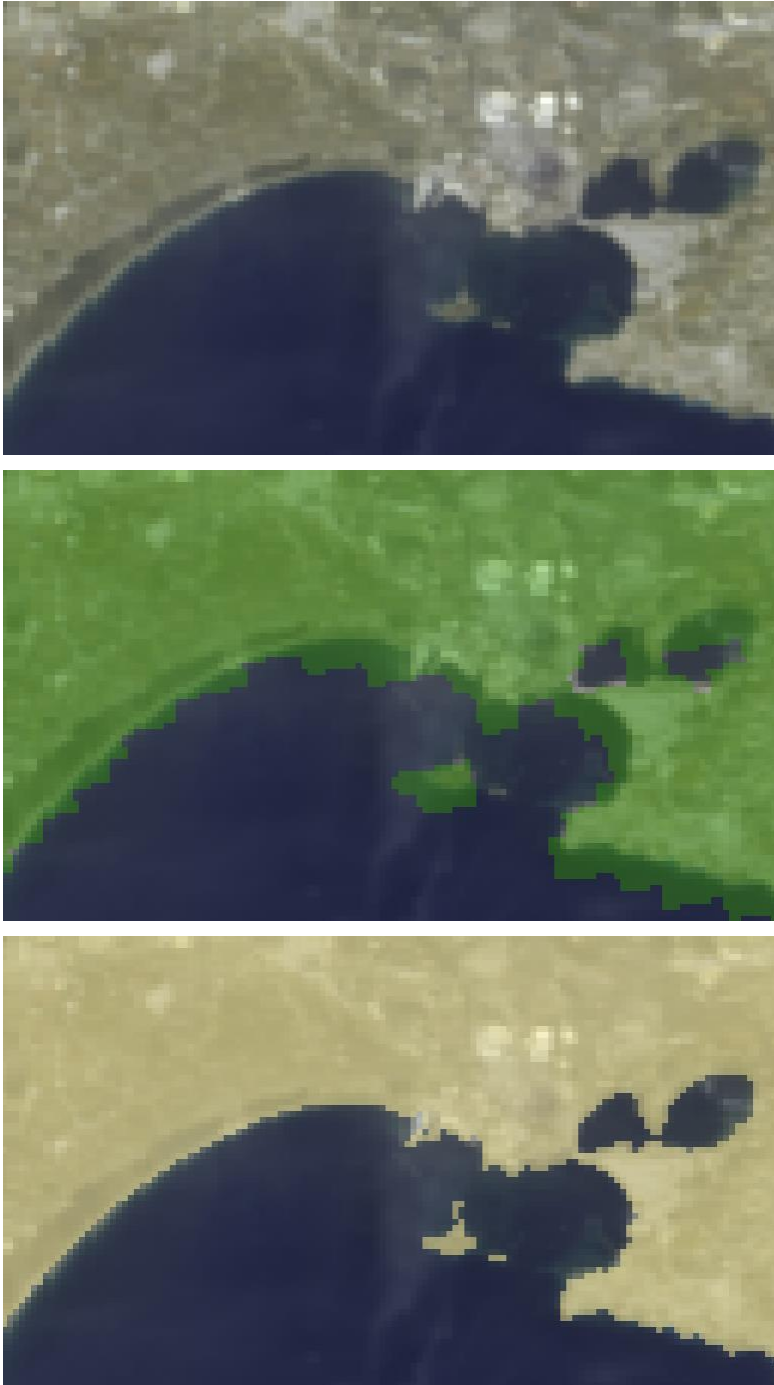


Figure 4: Land-water masks. Top: Top of atmosphere radiance RGB. Middle: TOA radiance RGB overlaid with the standard L1b cloud mask. Bottom: TOA radiance RGB overlaid with the Coastcolour land-water mask.

### 5.1.2 Cloud masking

The performance of the cloud masking is demonstrated at the example below for the Mediterranean Sea. This is a difficult case due to its large area of sun glint, including some small clouds over glint, and the field of thin clouds south-east of Italy. Visually the cloud screening of all types of clouds, i.e. the opaque clouds in the Adriatic sea, the thinner clouds in the southern Adriatic and the Greek coast, the thin clouds off Italy works well. Also, the glint area is not flagged as cloud but the clouds next to the glint and over glint (just offshore Lybia) are correctly flagged. A close look at the thin clouds off Italy is provided in Figure 6. The top left image shows the RGB which demonstrates the

different level of transparency of these clouds. The top right image shows the clouds flagged in white which seems to work well. The bottom left image masks the clouds in black and thin reveals a very slight increase of the brightness of the blue ocean next to the cloud. These are cloud borders that are not masked. CoastColour L1P provides a cloud buffer flag. This grows artificially the detected clouds by masking an area of  $n \times n$  pixels around every detected cloud pixel.  $n$  is a user supplied parameter with default = 1. The bottom right figure shows the effect of also masking the cloud buffer in black: the bright fringe disappears. Of course, this results in less clear sky pixels.

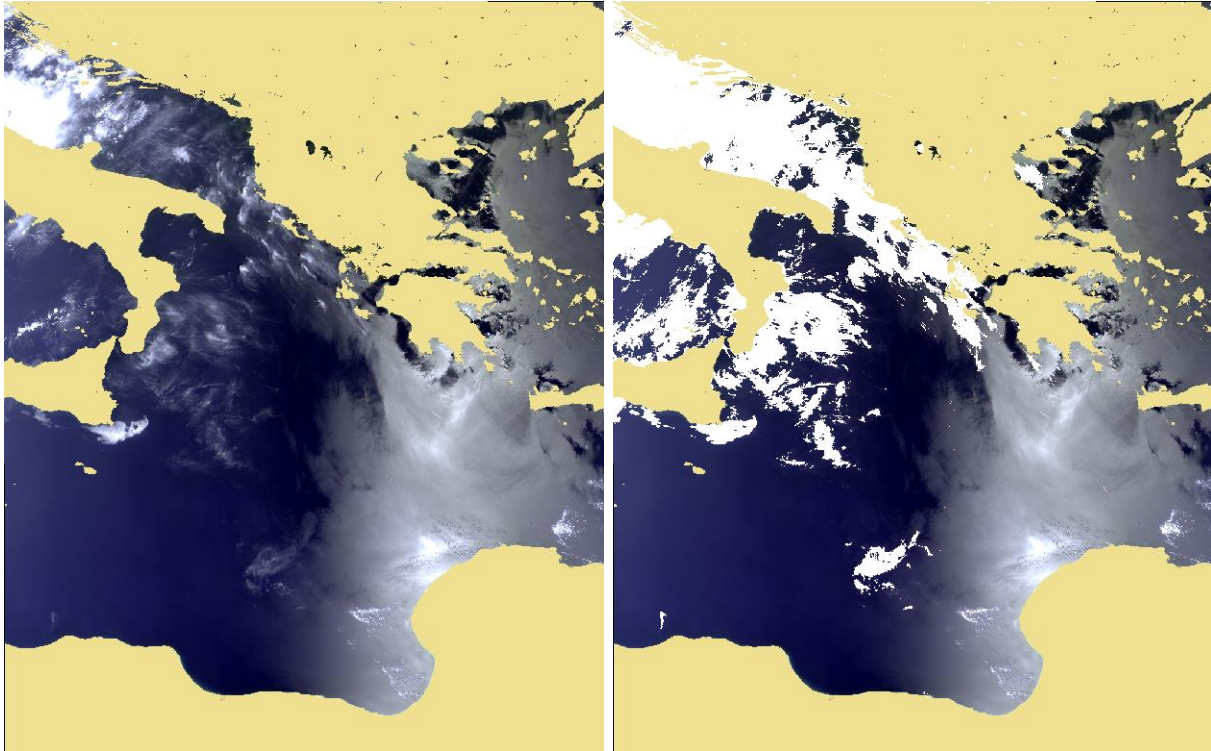
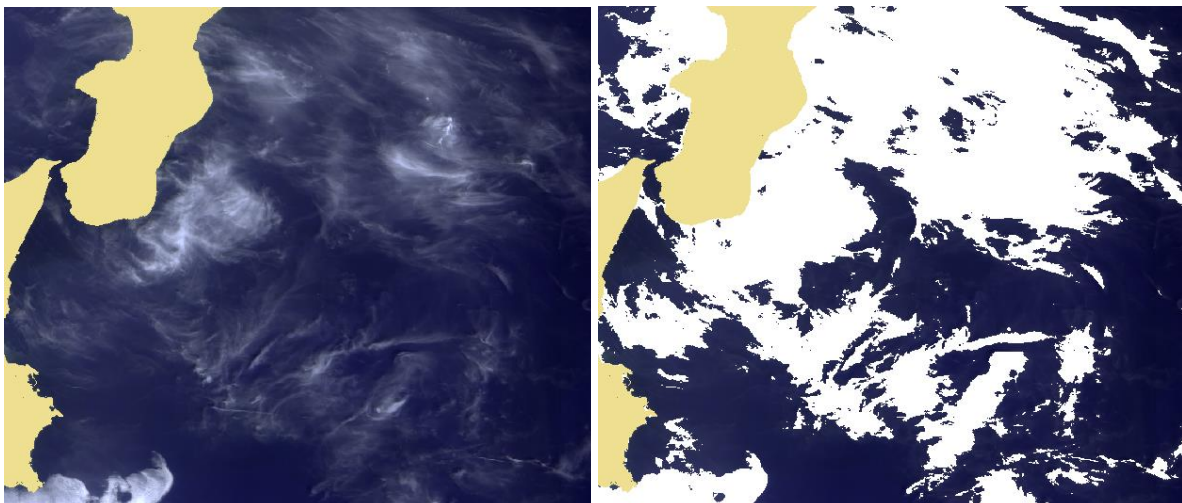


Figure 5 Demonstration of the cloud mask over the Mediterranean Sea. Left: TOA radiance RGB; right: TOA radiances overlaid with the cloud mask.



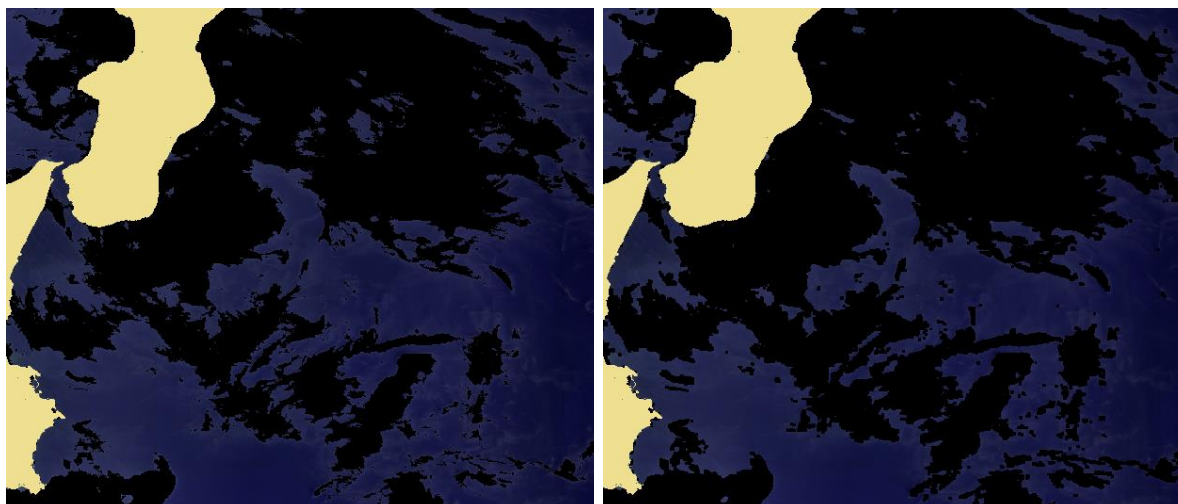


Figure 6: Subset of Figure 5 with thin clouds. Top left: TOA radiances RGB, top right: TOA radiances with clouds overlaid in white. Bottom left: cloud overlay in black. Bottom right: cloud and cloud buffer, overlay in black

The result of the quantitative analysis using the PixBox dataset and methodology is presented in Table 1 below. The overall performance of 85% is good. More important is the excellent performance of the cloud screening, where 99% of the true cloudy pixels (PixBox) are detected and flagged as clouds (producers accuracy). Most of the remaining 1% of not cloud flagged pixels are flagged as snow/ice, i.e. this is a mis-interpretation of the white signal, which is not harmful from an ocean colour point of view. The true snow/ice pixels are mostly classified as clouds (2746 pixels) and only 29% or 1124 pixels are correctly detected as snow/ice. This is due to less favourable bands for snow detection of MERIS, which is lacking a SWIR band. However, also this is not harmful from an ocean colour point of view. Only 2 snow/ice pixels are classified as water. Overall we can conclude that a Level 3 product will hardly be contaminated by undetected clouds. The number of valid water pixels which go into such a Level 3 is often sacrificed by an excellent cloud screening indeed suffer a bit. 84% of the water pixels are identified as such whereas 16% are misclassified as clouds. At CC Level 2 products this is taken into account by performing the atmospheric correction and in-water retrieval under ambiguous clouds, i.e. if the user has the chance to relax the strength of the cloud screening and obtain more pixels with water products.

The users accuracy is excellent for water pixels. 100% of the pixels classified by L1P as water are true water pixels. This is most important number of the users accuracy figures.

Table 1: Result of the cloud masking quality assessment (confusion matrix)

		PixBox			users accuracy
		water	cloud	snow/ice	
L1P	water	5433	23	2	100%
	cloud	1033	15068	2746	80%
	snow/ice	2	66	1124	94%
producers accuracy		84%	99%	29%	85%

## 5.2 L2R products

### 5.2.1 Match-up analysis

The basis of the validation of the CoastColour atmospheric correction is the match-up analysis with above water in-situ radiometric measurements. Such measurements are difficult to make and require to strictly following a certain protocol (e.g. MVT protocol). The best quality and best documented dataset is the MERMAID match-up database. However, this database does not include extreme turbid waters and most samples (95%) are from clear to moderately turbid water conditions. Moderately turbid waters here means a chlorophyll concentration of below 15mg/m<sup>3</sup> and a TSM concentration of below 15g/m<sup>3</sup>. This is not a severe limitation since most coastal waters are in this range, however, it does point properly the strength of the CoastColour atmospheric correction (CC-AC) which is to perform equally well for moderate and highly turbid waters. The highly turbid water is addressed in the next sub-section.

The overall performance of the CC-AC is shown in Figure 7, left, where it is also compared with the standard ESA atmospheric correction. All data with a valid retrieval from all MERMAID stations are included in this plot except the very clear waters which are not in the scope of CoastColour. The different colours represent the different spectral bands. The correlation coefficient is very high (0.90) and the data are well on the 1:1 line (gain=0.905, offset=-0.187). Two of the MERMAID stations are of very high quality, namely the Alta Aqua Ocean Tower, AAOT, in the northern Adriatic Sea. AAOT is half of the time in Case2 water conditions, and half of the time in Case 1 conditions. The result of the match-up analysis is shown in the right column of Figure 7. The correlation coefficient is slightly higher than for the global average, and also the slope and intercept of the regression line are close to the 1:1 line for AAOT than for the global average.

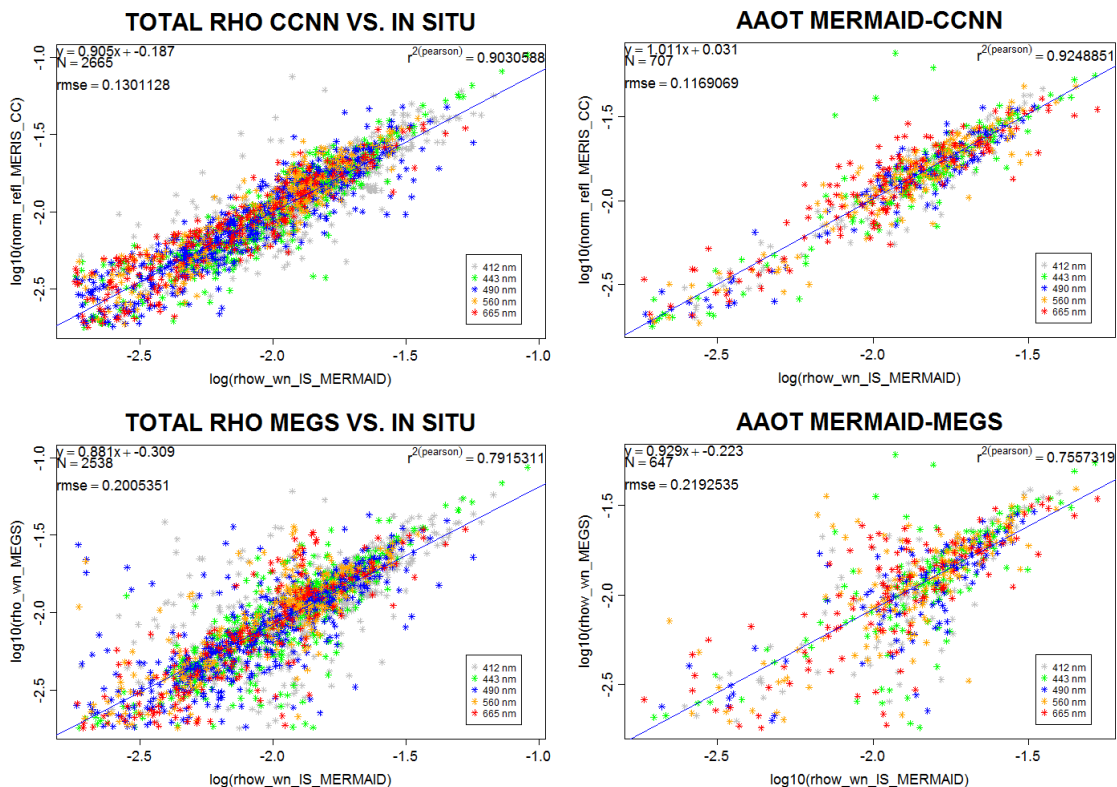


**Figure 7: Match-ups of water leaving reflectance with MERMAID water leaving reflectances for MERIS bands at 412nm, 443nm, 490nm, 560nm and 665nm (indicated by colours). Top left: CoastColour L2R, all sites in one plot, Bottom left: for comparison the standard MERIS L2 water leaving reflectance. Top right: same as top-left but only for measurements at site AAOT, Northern Adriatic Sea. Bottom right: same as bottom left but for AAOT.**

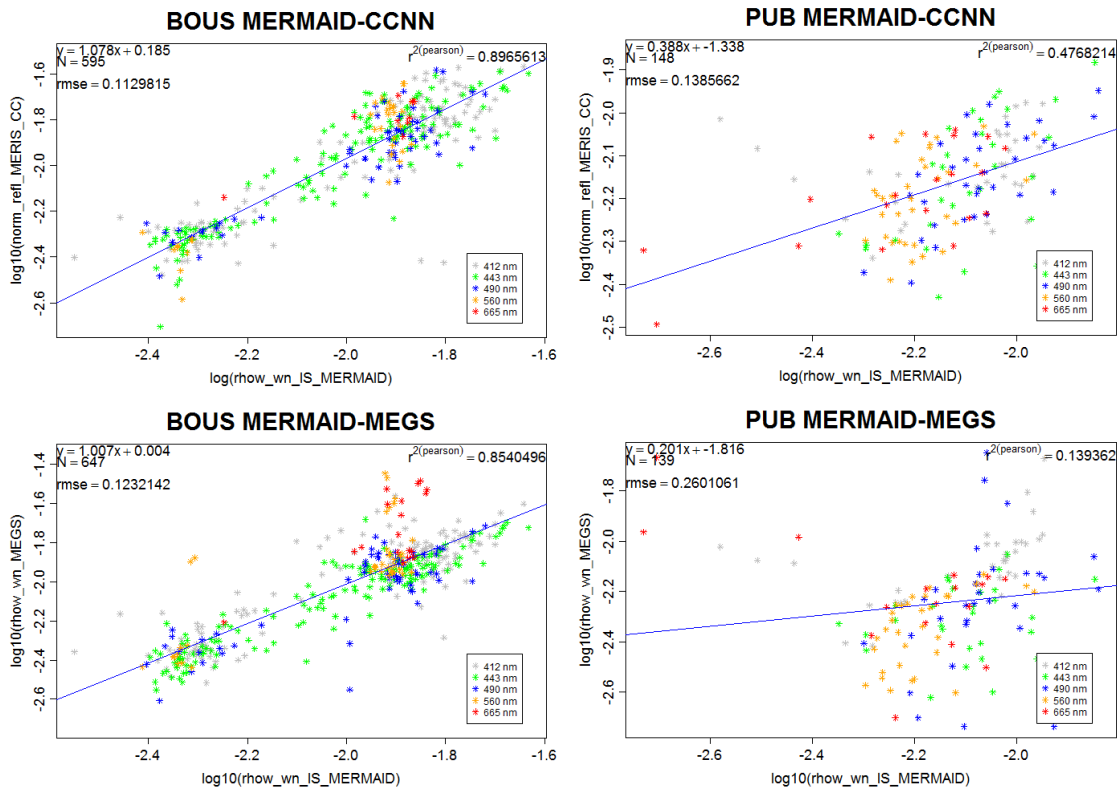


Figure 8: Same as figure Figure 7, right column, but here for site Boussle (left), a clear water site in the Mediterranean Sea, and Plumes and Blooms on US West coast (right, turbid station).

The case of a Case-1 water station, Boussle, is shown in Figure 8, left images. The performance here is not as good as for the coastal AAOT station, but it is as good as the global regression. The RMSE is slightly improved (0.11 for Boussle versus 0.13 for total), but the regression is almost equal to the total one (regression coefficient 0.896 versus 0.903).

The station Plumes and Blooms, which is located in the equally named CoastColour site 8 and which is characterised by relatively high sediment loadings, performs reasonably well, and the CC-AC improves the situation as compared to the standard product. The number of valid match-ups is only ~30 which is rather small<sup>5</sup>. The RMSE is good with a value of only ~0.13, i.e. like the total one. The coefficient of regression is a bit worse than the total one (0.48) and visually there is more scatter around the regression line too.

Two examples of absorbing waters (Baltic Sea) are shown in Figure 9 for Gustav Dahlen Tower, which is located off Stockholm, and Helsinki Lighthouse, which is located in the Gulf of Finland. Both show a similar performance and a consistent regression line. The RMSE is 0.16 (Gustav Dahlen) and 0.14, which is slightly worse than the total average and the turbid cases. The coefficient of regression is 0.81 and 0.82, which is also slightly worse than the total and AAOT case (0.90), but better than the Plumes and Blooms. The regression line is closer to the 1:1 line as the one of Plumes and Blooms. A remarkable feature of the match-up analysis of the Baltic Sea sites is the increase of the scatter with decrease of the reflectance. This was not observed in the other cases and might be an effect of the high amount of yellow substance in Baltic Sea water. High yellow substance leads to a decrease of reflectances and this seems to cause more noise in the atmospheric correction.

<sup>5</sup> The number n in the plots denotes the sum of all points in these figures, i.e. for all 5 spectral bands. An n~150 corresponds to 30 match-ups. Not all bands are always in the in-situ data and hence n can be small than 5 x samples.

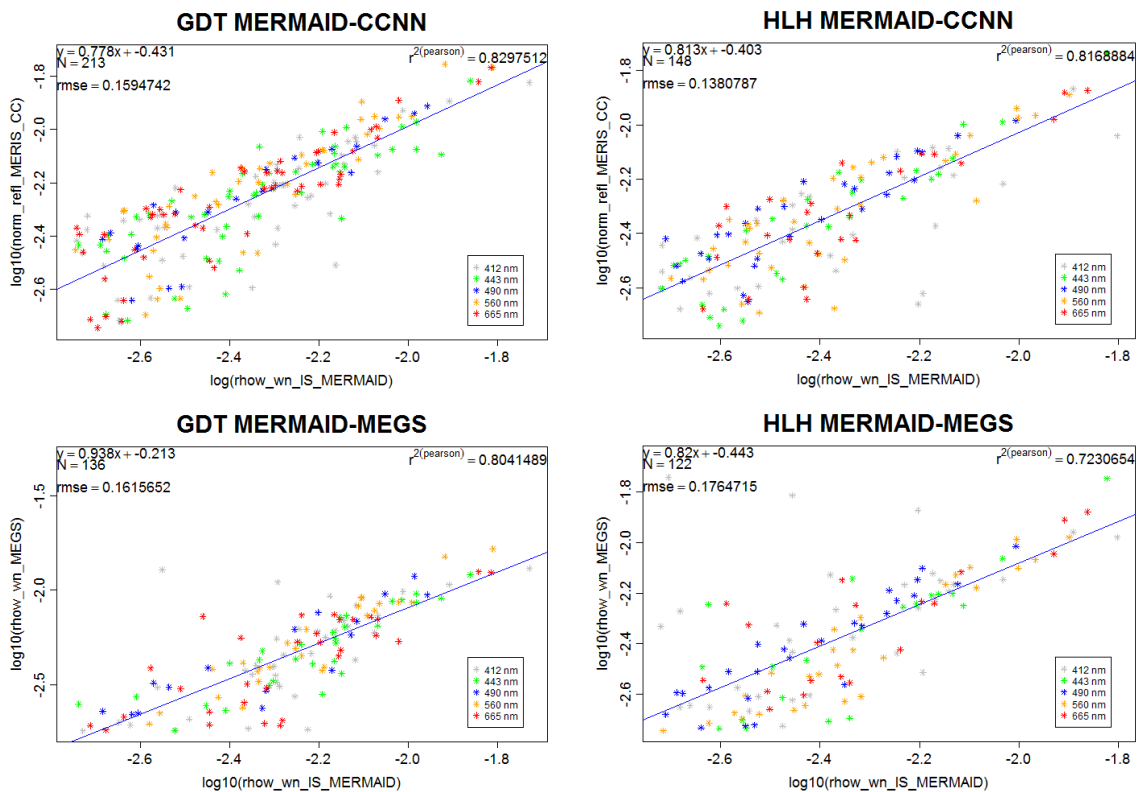


Figure 9: Same as figure Figure 7, right column, but here for stations Gutav Dahlen Tower (left), and Helsinki Lighthouse (right). Both sites are in absorbing waters in the Baltic Sea.

### 5.2.2 Performance for very high turbid waters

The MERMAID match-ups do not include many waters with TSM concentration above 15g/m<sup>3</sup> and the maximum concentration is at 25g/m<sup>3</sup> TSM. This is much lower than the range of the CoastColour bio-optical model, which goes up to 500g/m<sup>3</sup> in order to perform for cases like the Yellow River or the Rio de la Plata. TSM concentrations of this magnitude cause a significant backscatter in the NIR spectral bands and the atmospheric correction has to take this properly into account. Most standard atmospheric correction, such as the standard ESA AC or the SeaDAS l2gen of NASA, are not applicable to such waters. In this chapter we investigate the performance of the CoastColour AC for the Rio de la Plata, where the TSM concentration shows a gradient from clear water in the open ocean (TSM below 1g/m<sup>3</sup>) up to more than 250g/m<sup>3</sup> in the estuary of the river<sup>6</sup>. The turbidity maximum is clearly defined where the river water interacts with the clear shelf water, as shown in The water leaving reflectances reach values of 0.2, with the maximum located in the red part of the spectrum.

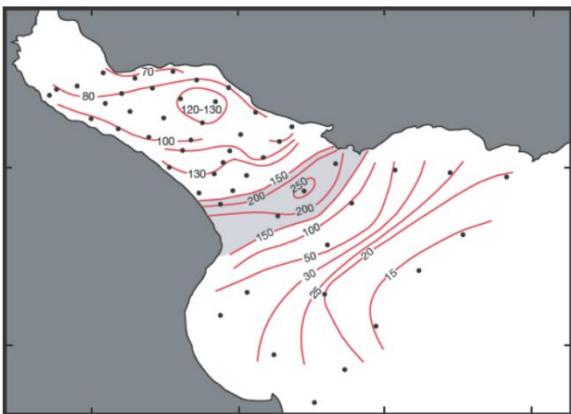


Figure 10. The water leaving reflectances reach values of 0.2, with the maximum located in the red part of the spectrum.

<sup>6</sup> Dogliotti et al, 2013, CoastColour UCM4, Darmstadt.

Figure 10: Mean surface suspended sediment concentration in Rio de la Plata (surveys 1981-1987), taken from Framinan, 1985

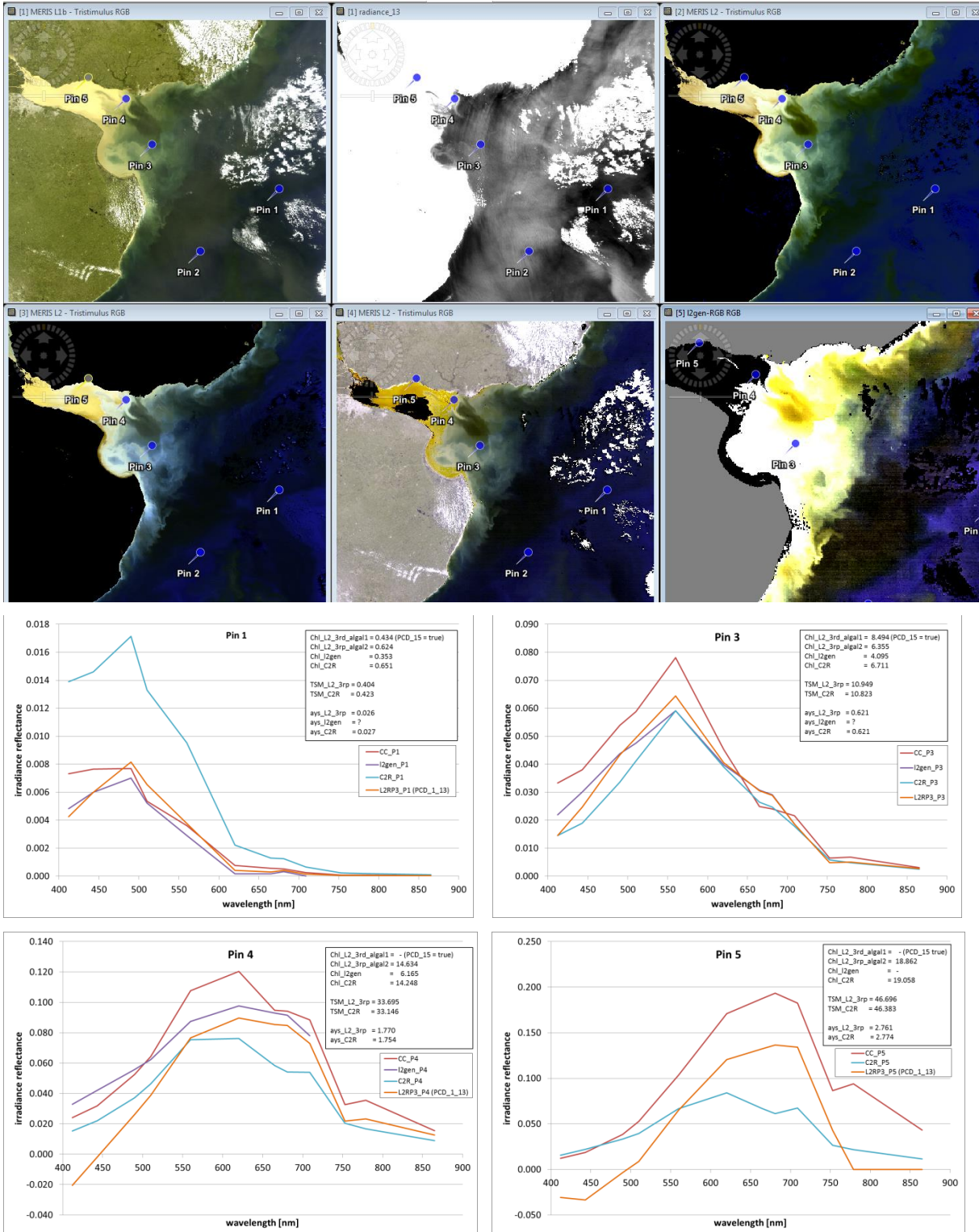


Figure 11: Comparison of the performance on different atmospheric correction for a large range of different sediment loadings, Rio de la Plata. Top 6 images showing the source image as RGB (top left), TOA radiance at 865nm (top centre), RGB of water leaving reflectance (wlr) with Case2R AC (top right), RGB of wlr with CoastColour AC (second row, left), standard ESA processing AC (second row, centre) and SeADAS I2gen AC (second row, right). The same 5 pixels are

marked with pins in each image, and the spectra at 4 of these 5 locations are shown in the lower 4 graphs (pin 2 is omitted because it does not add extra information).

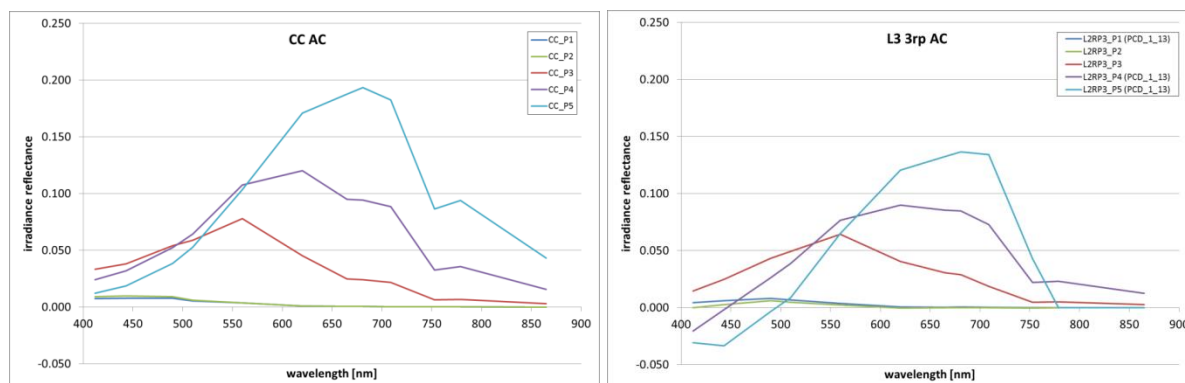


Figure 12: Comparison of the spectra at the selected pixels for the CoastColour AC (left) and the standard MERIS AC (right).

We will investigate the results of the CoastColour AC for this area and compare it with the performance of other atmospheric corrections currently available. Figure 11 shows in the top left image the TOA RGB image, with the dark blue water of the open ocean and the bright sediment loaded river water, mixing with the oceanic water. Also the river front is visible. The other 5 images of the 2 top rows of Figure 11 show RGB of water leaving reflectances obtained with the Case2R AC (top left), the CoastColour AC (2<sup>nd</sup> row, left), standard ESA AC (2<sup>nd</sup> row, centre) and NASA I2gen AC (2<sup>nd</sup> row, right). 5 pixels are marked with Pins, which can be best seen in the top row, centre image, which shows the TOA signal in the NIR at 865nm in the background. At 4 of these 5 pixels the water leaving reflectance spectra are compared and shows in Figure 11 bottom rows.

Pin 1 is located in the open ocean and shows a typical clear water spectrum. All ACs except the Case2R perform very similar. Differences exist for band 1 where the CoastColour AC has a higher signal compared to the others. For information the retrieved water constituents are shown in the inset. For this pixel all processors retrieve a chlorophyll concentration around 0.5mg/m<sup>3</sup> and a TSM concentration of also ~ 0.5g/m<sup>3</sup>.

Pin 3 is located closer to the mouth of the river in an area where the influence of the river water is clearly visible in the TOA RGB. According to Framinan, 1985 (Figure 10) the TSM concentration should be in the order of 20g/m<sup>3</sup>. The spectra of all ACs agree very well in their shape. The CoastColour AC has slightly higher values than the other three for the short wavelength bands. The TSM concentrations retrieved are ~ 10g/m<sup>3</sup>.

Pin 4 is located in the mixing zone of the river water with the ocean water. The spectra are getting a sediment dominated shape (high reflectances) but also with substantial amount of chlorophyll absorption in the blue. All spectra show similar shape. Only the CoastColour AC is still able to show the increase in the red reflectances at an expected amount (~0.1 at 665nm). The other ACs are at the limit of their definition range here. The standard L2 AC is no longer able to correct the high scattering in the NIR and overinterprets it as aerosol. This lead to an overcorrection in the blue and consequently negative reflectances in bands 1 and 2. The spectrum is correctly flagged as invalid.

Pin 5 is located at the maximum reflectance within this image. The standard ESA product and the NASA I2gen AC do not provide valid water leaving reflectances (flagged, negative reflectances). The Case2R AC provides the right shape of the spectrum but does not reach the expected reflectance level of 0.2 in the red/NIR but remains at a level below 0.1, which seems to be the maximum that was included in its training range. Only the CoastColour AC provides the correct shape, including a typical peak in the NIR, and reaches a reflectance level of 0.2 at 665nm.

Figure 12 presents the spectra at all 5 pins in one plot for the CoastColour AC (left) and the standard MERIS AC (right). One can see the evolution of the spectrum from clear water (blue and green curves) with low reflectances and the decrease from blue to red, to the turbid round shape. It can

also been seen very nicely how the maximum of the spectrum increases and shifts towards red/NIR with increase of TSM (indicated by increase of Pin number). The standard MERIS AC and the CoastColour AC perform very similar for the first 3 pins but then the standard AC misinterprets the NIR reflectances, overcorrects in the blue and does not reach the high reflectance values in the red/NIR.

### 5.2.3 Glint correction

The performance of an atmospheric correction in the presence of sun glint is important in order to maximise the number of valid retrievals. This is the case in particular for MERIS which is significantly impacted by sun glint. Since in-situ observation under sun-glint conditions are sparse (in-situ campaigns are planned such that the observation conditions are optimal and hence glint will be avoided) one mean to investigate the performance of the AC under glint conditions is to study the stability of the water leaving reflectance across track for an area where the water constituents do not vary much. The test case shown in Figure 13 is the Mediterranean Sea south of Italy and Greece. Half of the orbit is affected by sun glint. Data before and after atmospheric correction were extracted along a transect which is shown as red line in the image.

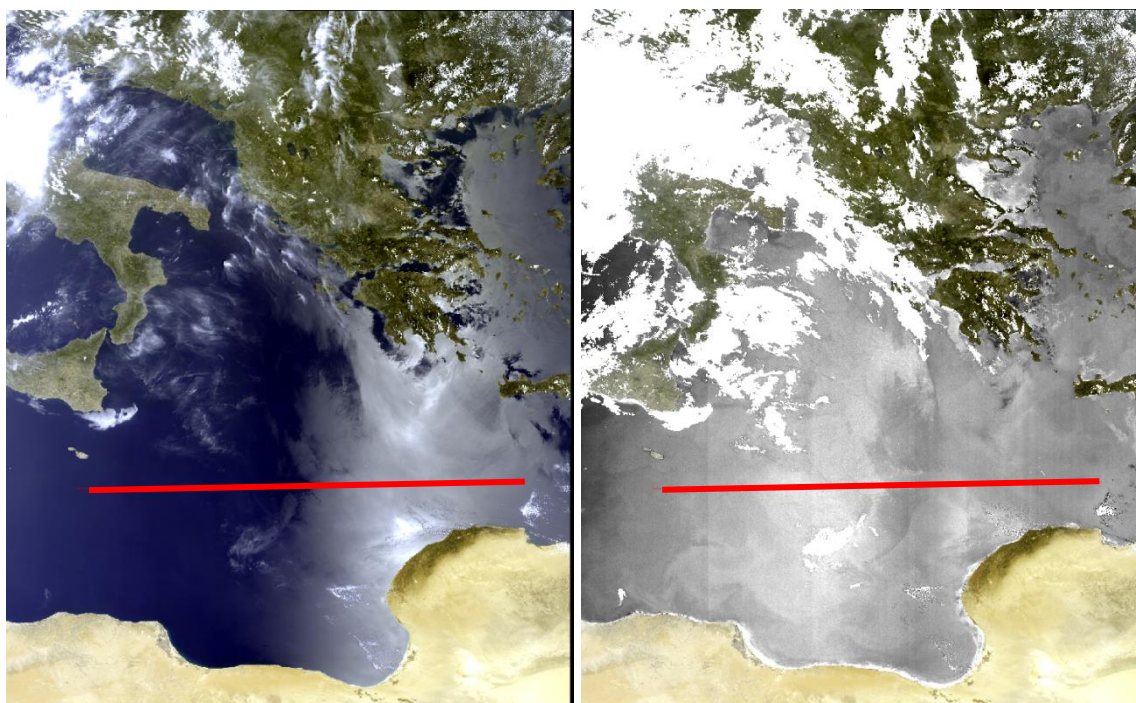


Figure 13: MERIS scene of 19.05.2006. Left: top of atmosphere RGB with the location of the transect shown as red line. Right: water leaving reflectance in band 3 (490nm).

The top graph of Figure 14 shows the TOA radiance in band 3 (490nm). The signal is starting at  $60 \text{ W/m}^2 \text{ sr nm}$  and slightly decreasing down to  $50 \text{ W/m}^2 \text{ sr nm}$  in the centre of the transect. Here the influence of the sun glint is clearly visible with an increase of the signal to  $110 \text{ W/m}^2 \text{ sr nm}$  at pixel 2500 along the transect, followed by a decrease down to  $90 \text{ W/m}^2 \text{ sr nm}$  towards the end of the transect.

The bottom graph of Figure 14 shows the water leaving reflectance in band 3 along this transect. The signal is rather stable at a level of 0.02 with some variation along the transect, and it is independent from the glint signal. Most remarkable is the increase from the western end of the transect towards the centre. The glint peak shape in the eastern part of the transect is not occurring at all in the water leaving signal. However, the rapid change from the maximum value of the water leaving reflectance at pixel 1750 down to the 0.2 level coincides with the steep increase due to the glint. From these data alone one cannot say if this is by accident or if there is a systematic relationship.

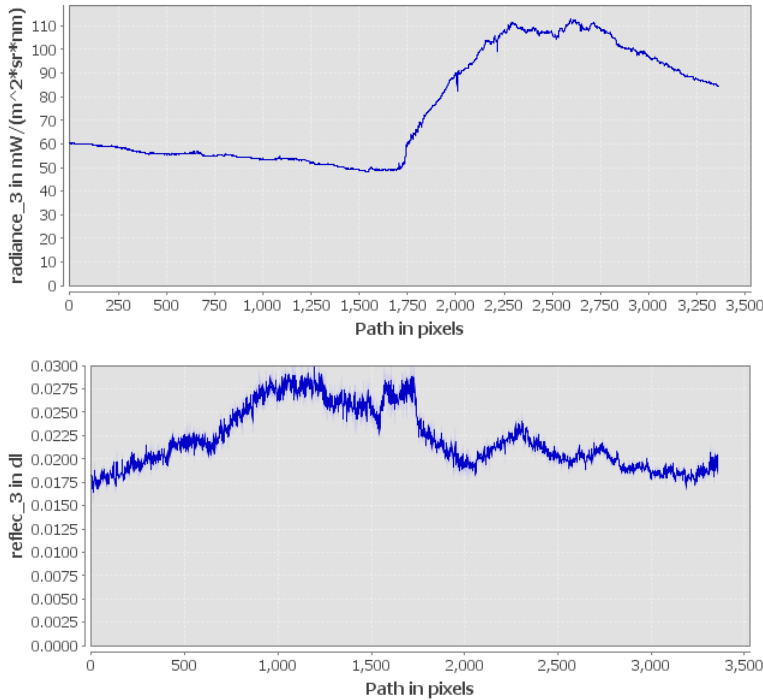


Figure 14: top: TOA radiance in band 3 (490nm) radiance along the transect. Bottom: water leaving reflectance in band 3 (490nm) along the transect.

### 5.3 L2W products

Several dependent variables are plotted against the independent variable to see how they are correlated. The independent variable ( $x$ ) considered changes being chlorophyll concentration, total suspended matter or yellow substance absorption measure by the in situ data. The dependent variables ( $y$ ) are the chlorophyll, TSM and IOPs calculated with the Coast Colour neural net on the 3<sup>rd</sup> reprocessing full resolution MERIS archive. There are two in situ datasets taken as reference, as explained in section 4.1.2, namely the CoastColour and the MERMAID in-situ data.

**The CoastColour in situ dataset is used as reference data to compare with the results of the NN. Table 2 and**

When referring to TSM, the coefficient of determination seems to be lower than the chlorophyll values, but the correlation is clearly visible. Site 4 (Morocco) was removed from the calculation of the total TSM correlation because of the behaviour of the measurements differed obviously from the rest of the data in this dataset (see Figure 18 with the plot by site 4). There are other two outliers in site 25 (Tasmania), which have been removed as well (see Figure 18 with the plot by site 25).

The YS parameter is a bit more scarce and complicated to find data and matchups. With only 15 matchups, all in site 3 (Mediterranean and Black Sea), to derive some conclusion is quite complicated. Coefficients of determination are low, but also the RMSE are low in both comparisons. The parameters compared are a bit different as well: CDOM fluorescence versus inherent optical properties (absorption of CDOM -iop\_a\_dg\_443- and absorption of yellow substance -iop\_a\_ys\_443).

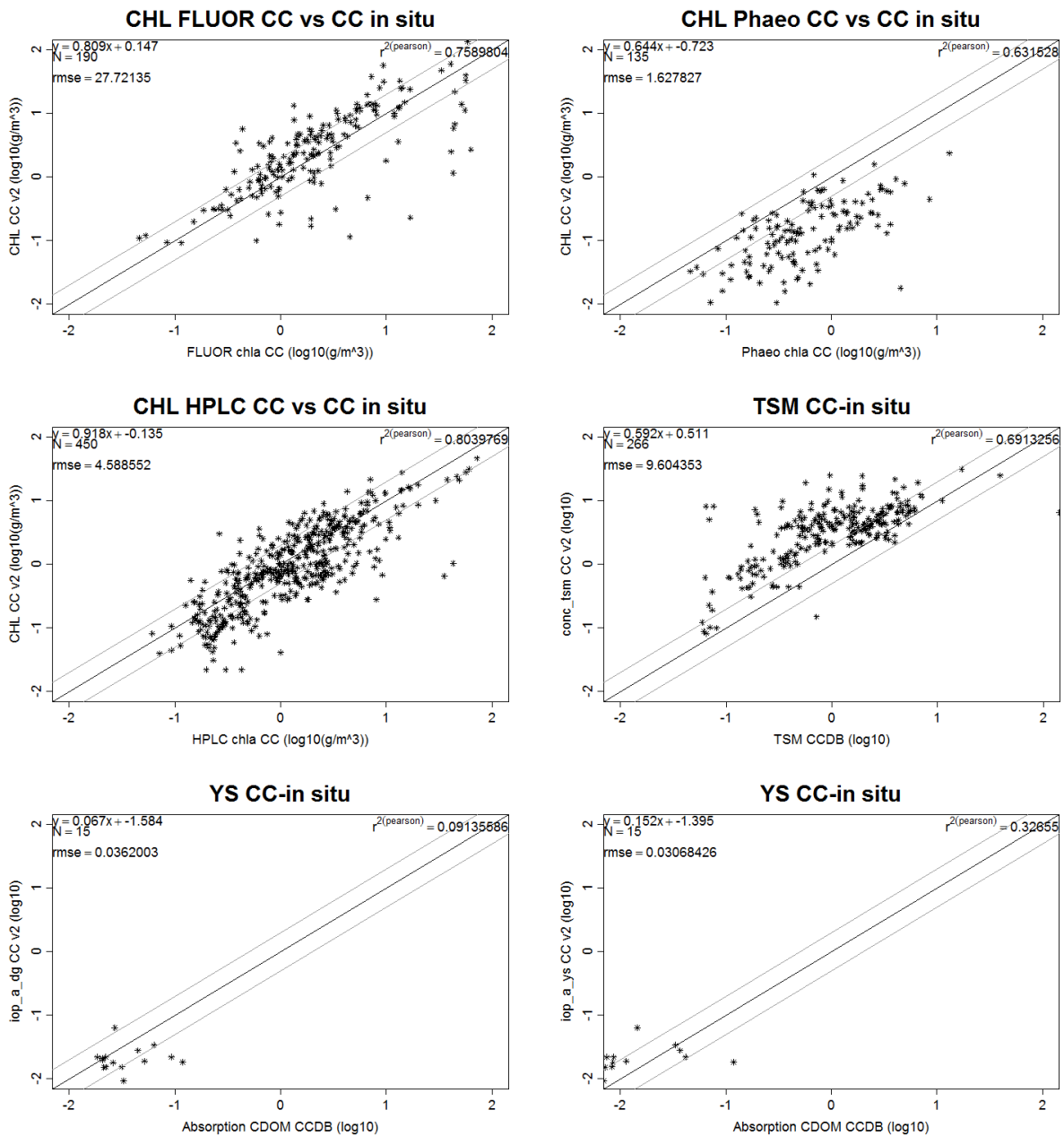


Figure 15 show the total results of the different comparisons by parameter. The CC chlorophyll (merged algorithm) is compared with in-situ chlorophyll derived by 3 different methods: flourometric method, HPLC and Phaeo-pigments

All three methods show good correlations with the CC choropyll merged algorithm. However, the flourometric method has a high root mean squared error (27.72 log10(g/m<sup>3</sup>)), that seems to be introduced by the data of site 20 (Central California). See Figure 16 and Figure 17 for details about the behavior of the chlorophyll concentrations by site/method. Using the HPLC method, the best correlations are found in site 4 (Morocco), site 26 (Gulf of Mexico) and site 1 (North Sea). Using the flourometric method, best data are from site 7 (Oregon and Whashington), site 11 (China, Korea, Japan) and site 20 (Central California).

**Table 2 Statistics of the linear regressions (Coast Colour in situ dataset)**

Linear regression	Coefficients		Root mean squared error	Coef of determination r-squared	Number of samples	Coefficient of correlation
	Intercept	Slope				
FLUOR_chla_IS vs chl_conc_merged	0.147	0.809	27.721	0.759	190	0.871
Phaeo_IS vs chl_conc_merged	-0.723	0.644	1.628	0.631	135	0.795
HPLC_chla_TOTAL_IS vs chl_conc_merged	-0.135	0.918	4.59	0.804	450	0.897
a_g_IS_443 vs iop_a_ys_443	-1.395	0.152	0.031	0.326	15	0.571
a_g_IS_443 vs iop_a_dg_443	-1.584	0.067	0.036	0.091	15	0.302
TSM_IS vs conc_tsm (without site 4)	0.511	0.592	9.604	0.691	266	0.831
TSM_IS vs iop_b_tsm (without site 4)	0.719	0.295	7.258	0.692	266	0.832

When referring to TSM, the coefficient of determination seems to be lower than the chlorophyll values, but the correlation is clearly visible. Site 4 (Morocco) was removed from the calculation of the total TSM correlation because of the behaviour of the measurements differed obviously from the rest of the data in this dataset (see Figure 18 with the plot by site 4). There are other two outliers in site 25 (Tasmania), which have been removed as well (see Figure 18 with the plot by site 25).

The YS parameter is a bit more scarce and complicated to find data and matchups. With only 15 matchups, all in site 3 (Mediterranean and Black Sea), to derive some conclusion is quite complicated. Coefficients of determination are low, but also the RMSE are low in both comparisons. The parameters compared are a bit different as well: CDOM fluorescence versus inherent optical properties (absorption of CDOM-iop\_a\_dg\_443- and absorption of yellow substance -iop\_a\_ys\_443).

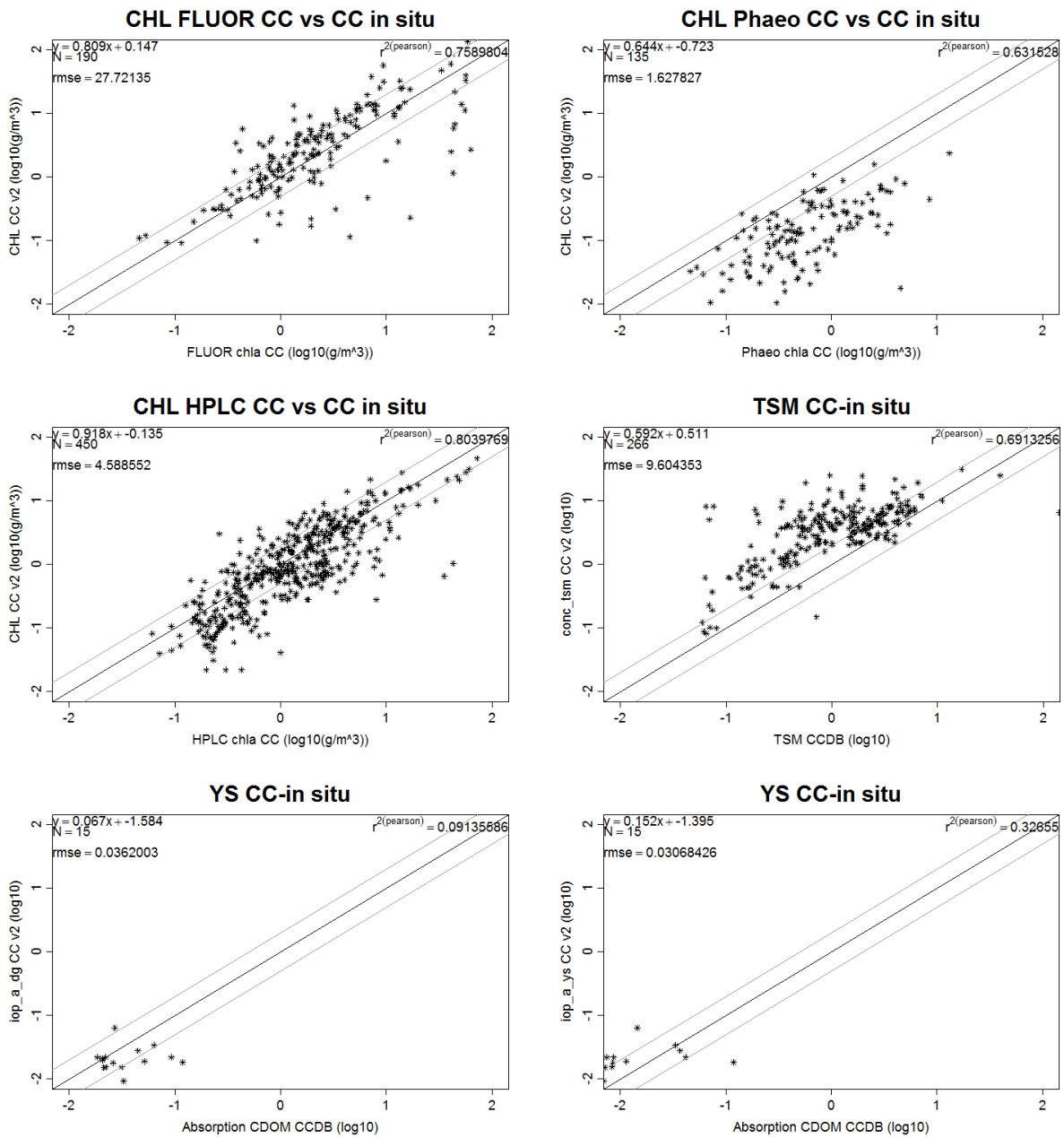


Figure 15 Linear regression with coefficients between the total chlorophyll concentration, TSM and YS extracted with the CC neural net and several chlorophyll\_a in situ measurements (FLUOR, HPLC and Phaeo), TSM concentrations and YS absorption, in log scale

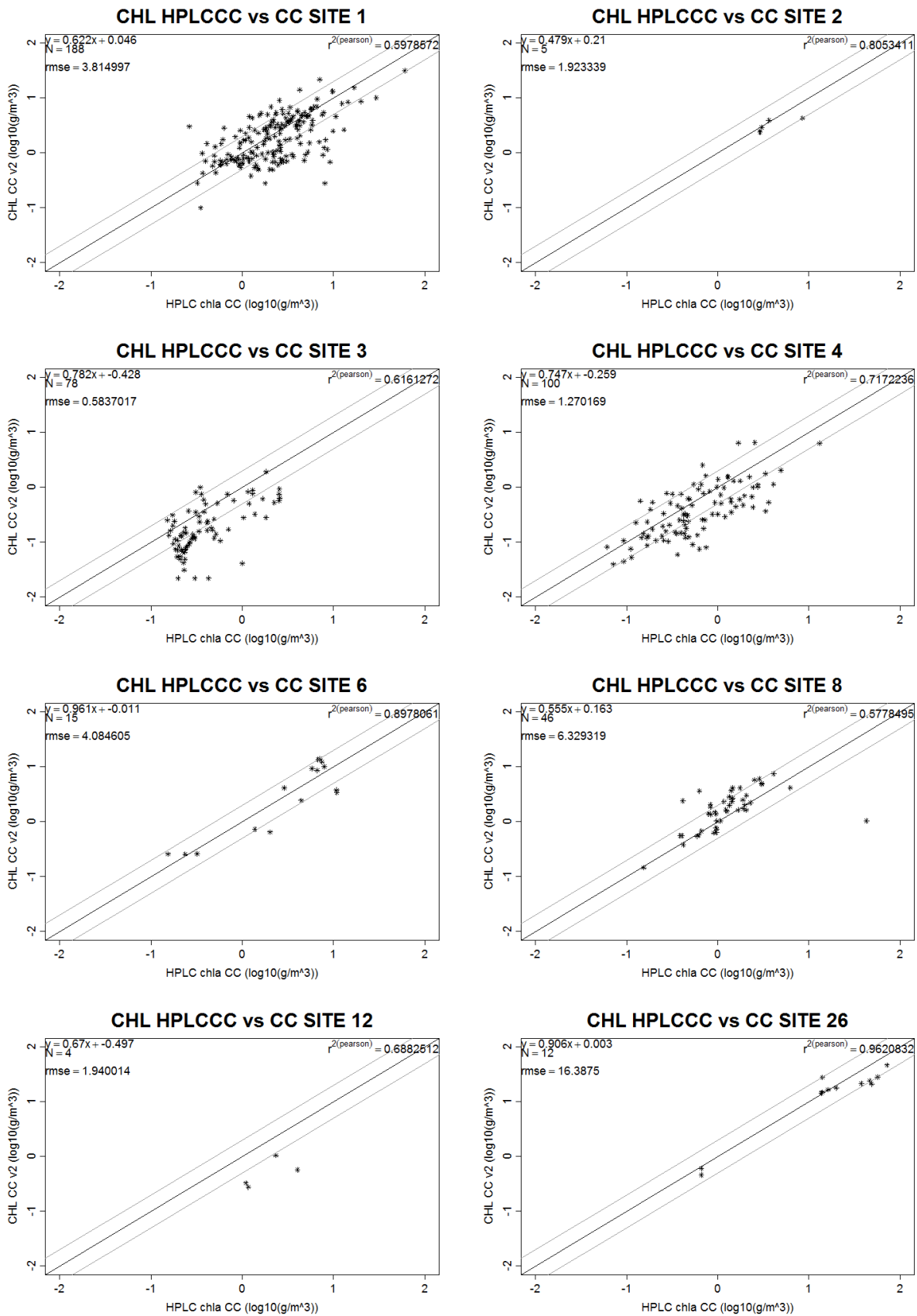


Figure 16 Linear regression with coefficients between the chlorophyll concentration and the HPLC method by CC site, in log scale

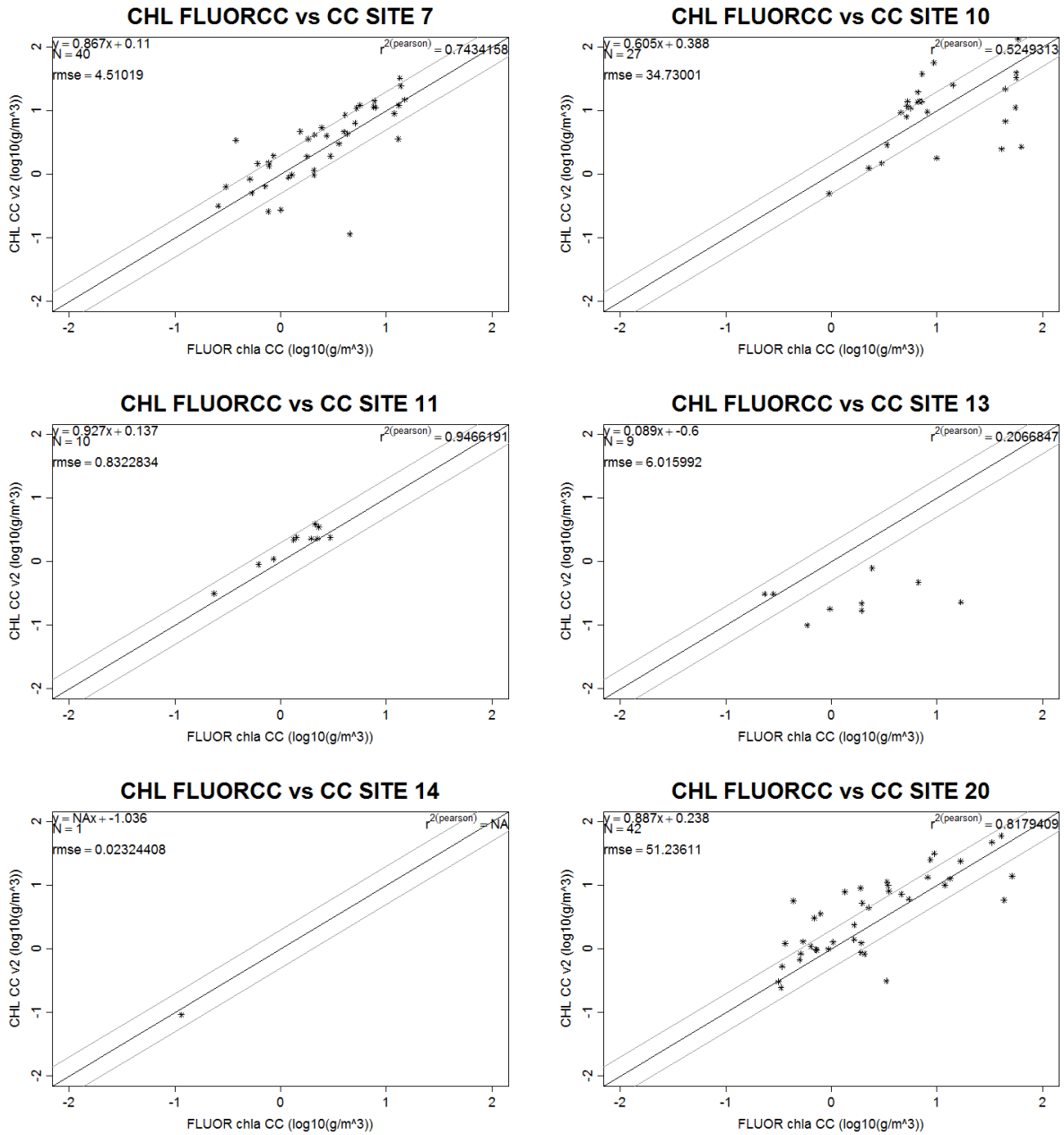
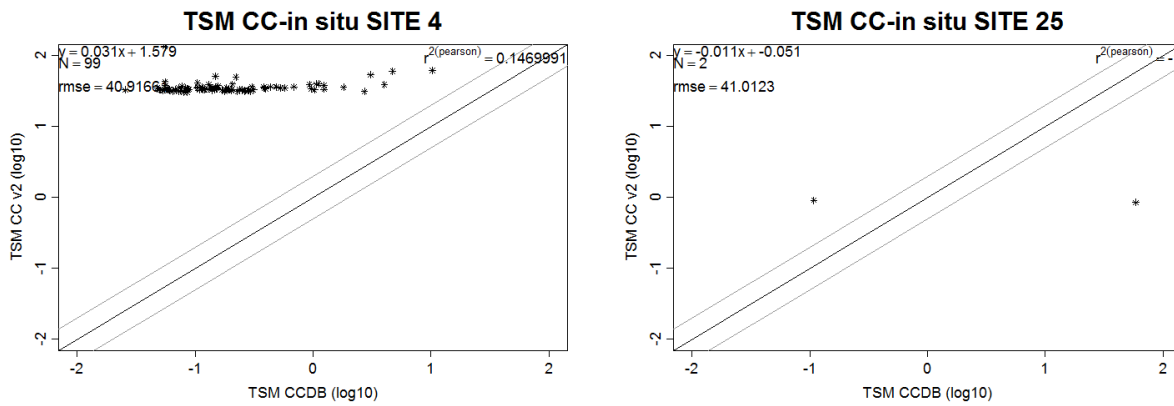


Figure 17 Linear regression with coefficients between the chlorophyll concentration and the flouometric method by CC site, in log scale



**Figure 18 Linear regression with coefficients between the suspended matter concentration and the in situ TSM by CC site 4 and site 25, in log scale**

Concerning the Mermaid dataset, Table 3 shows a summary of the different quantities calculated from the regression analysis, in log10. The following figures show the scatterplots of the in situ versus the dependent variables (Figure 19 to Figure 21). The regressions show in general good coefficients of correlation for the chlorophyll measurements with flourometric procedures and HPLC. The best coefficient of determination is found in the comparison of the CC chorophyll concentration and the flourometric measures, but the error is lower for the HPLC method that comprises the total chlorophyll\_a from HLPC pigment analysis (RMSE = 1.232 g/m<sup>3</sup>). The regression with spectrophotometric method counts with only four matchups, and cannot really be comparable to the others.

The regression of the absorption by yellow substance (Figure 20) measured with the in situ absorption values does not show such a high correlation coefficients, but the RMSE are very low for 52 samples. The total suspended matter comparison (Figure 21) gives good correlation with the in situ data (alghough only very few match-ups are available). Results are not so good for the comparison with the backscattering IOP (iop\_b\_tsm), but error keeps low. Still it seems to be an overestimation of the TSM concentration in the CC NN measures.

**Table 3 Statistics of the linear regressions (Mermaid matchup dataset)**

Linear regression	Coefficients		Root mean squared error	Coef of determination r-squared	Number of samples	Coefficient of correlation
	Intercept	Slope				
SPECT_chla_IS vs chl_conc_merged	-0294	0.426	1.138	0.746	5	0.863
FLUOR_chla_IS vs chl_conc_merged	0.205	1.018	4.797	0.877	99	0.936
HPLC_chla_ONLY_IS vs chl_conc_merged	-0.062	0.7758	7.224	0.647	192	0.804
HPLC_chla_TOTAL_IS vs chl_conc_merged	-0.05	0.99	4.873	0.886	236	0.941
a_g_IS_443 vs iop_a_ys_443	-1.058	0.169	0.196	0.281	137	0.530
a_g_IS_443 vs iop_a_dg_443	-1.119	0.135	0.491	0.192	137	0.439
TSM_IS vs conc_tsm	-0.05	1.523	6.830	0.444	50	0.666
TSM_IS vs iop_b_tsm	0.016	0.379	4.955	0.244	50	0.494

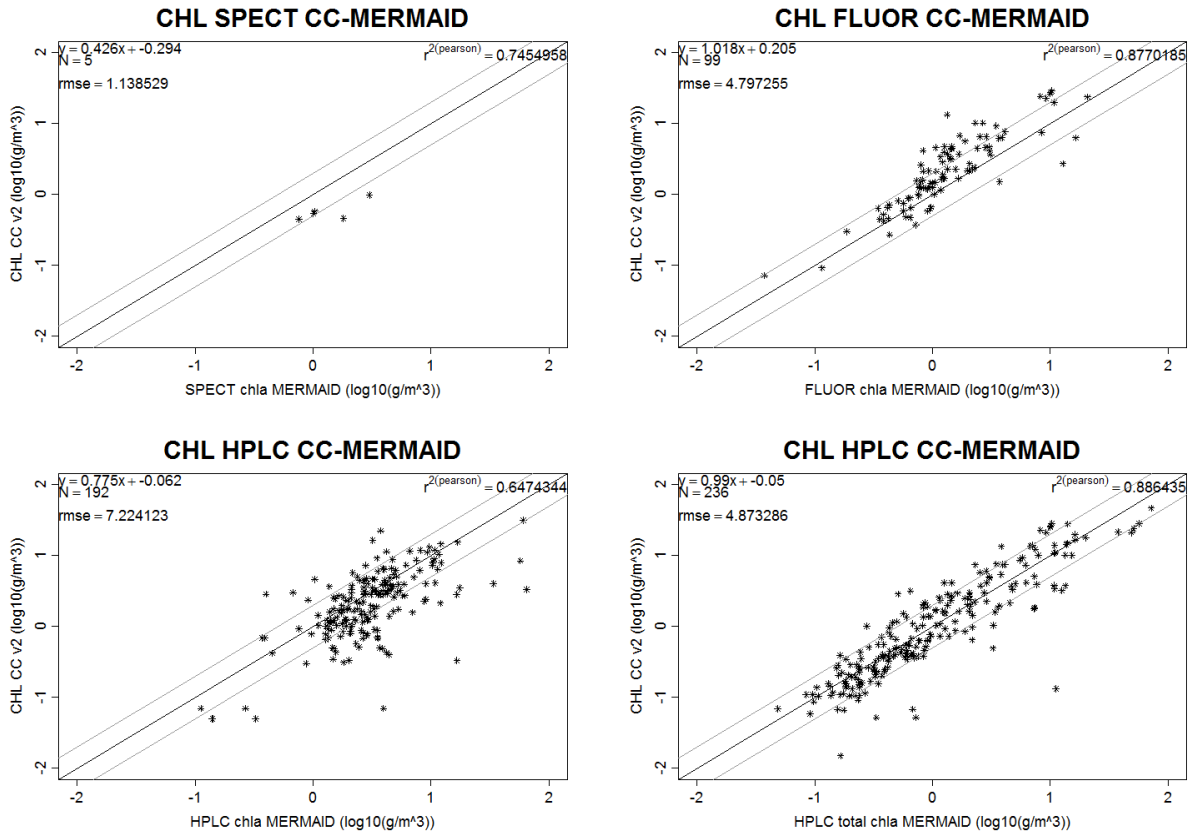


Figure 19 Linear regression with coefficients between the chlorophyll concentration extracted with the CC neural net and several chlorophyll\_a in situ measurements (SPECT, FLUOR, HPLC derived only from pigmet analysis and HPLC total), in log scale

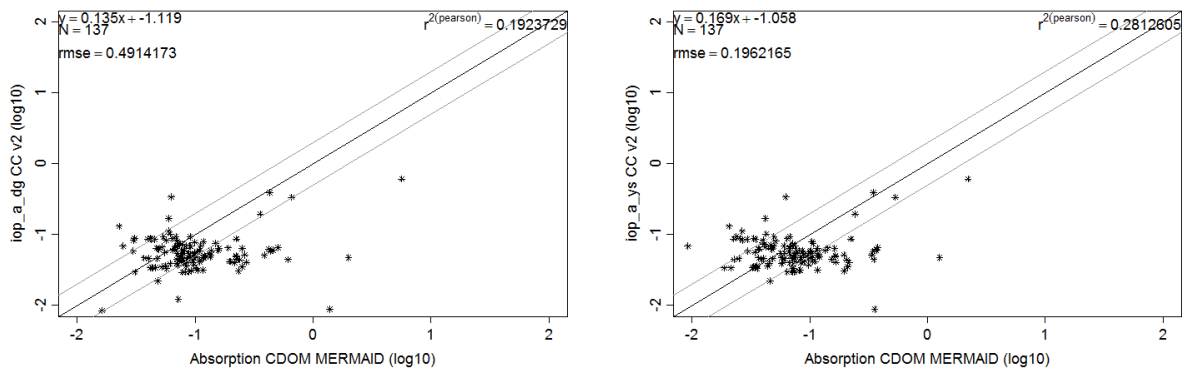


Figure 20 Linear regression with coefficients between absorption of the yellow substance (right) and dg (left), and the absorption of CDOM from in situ measurements, in log scale

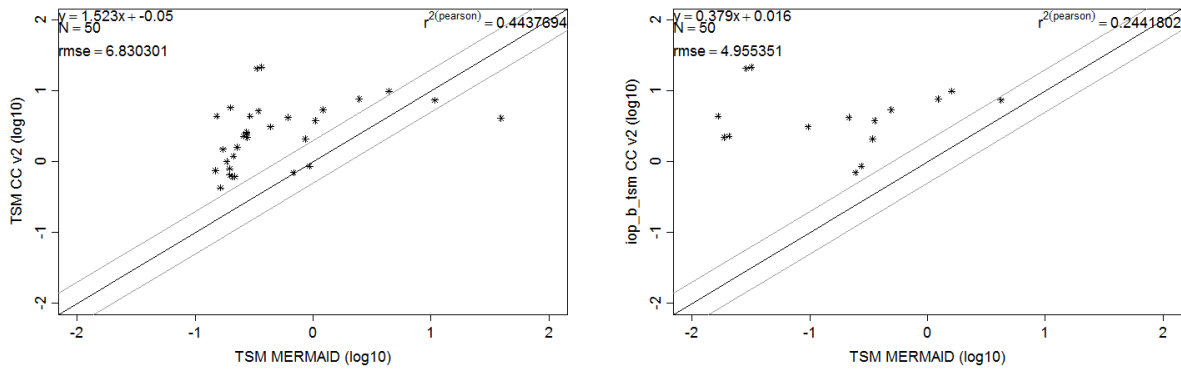


Figure 21 Linear regression with coefficients between the total suspended matter concentration from the CC neural net and the TSM measure in situ (left) and comparison with the backscattering value (right), in log scale

## 5.4 Case studies

### 5.4.1 North Sea and Western English Channel

A self-standing report has been produced by PML which is provided in the Annex to this report. This report was produced on the V1 products of CoastColour. The results presented here actually had lead to introducing the OC4 chlorophyll algorithm into the V2 processing of CoastColour. In this respect the results presented here, using L2R and OC3, corresponds for the concerned waters to the CoastColour V2 processing.

The objective of this report is to validate new MERIS derived Level 2 products to define the most accurate Ocean Colour (OC) chlorophyll-a (Chla) algorithm(s) for the INTERREG-2Seas areas of the North Sea and Western English Channel coastal areas (see Figure 22). The report uses full resolution (FR) COASTCOLOUR data with standard Chla (Algal Pigment 2 - AP2) and non-standard (OC3) algorithms to evaluate their potential use in the INTERREG-2Seas area.

The assessment resulted in the following conclusions:

- From a database of 529 sampling points for Chla from cruises in 2003 to 2009, there were N=35 match-ups at <45 mins from MERIS overpass. It is incredibly difficult to get a large number of high quality match-ups for the INTERREG 2-Seas area using conventional ship borne oceanographic sampling techniques
- From the few match-ups available, FR COASTCOLOUR MERIS Rrs at 490, 510, 560 and 665 nm were accurate to >0.3 Log<sub>10</sub> -RMS indicating that data at these wavebands can be used to produce potentially accurate Level 2W products. Rrs at 412 and 442 nm were less accurate and showed an inherent under-estimate at both low and high range Rrs values.
- Using FR COASTCOLOUR Level 2R, OC3 Chla was more accurate than the standard AP2 Chla

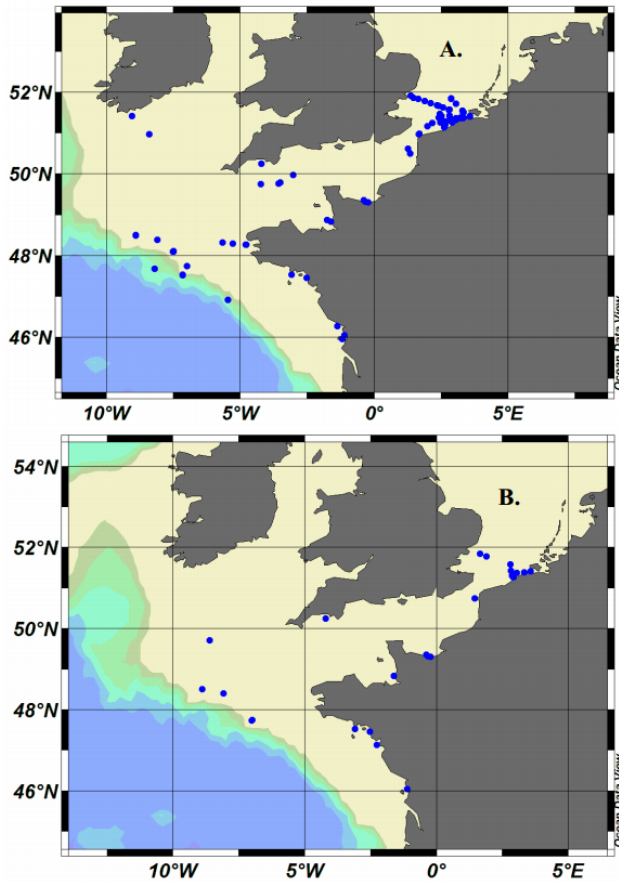
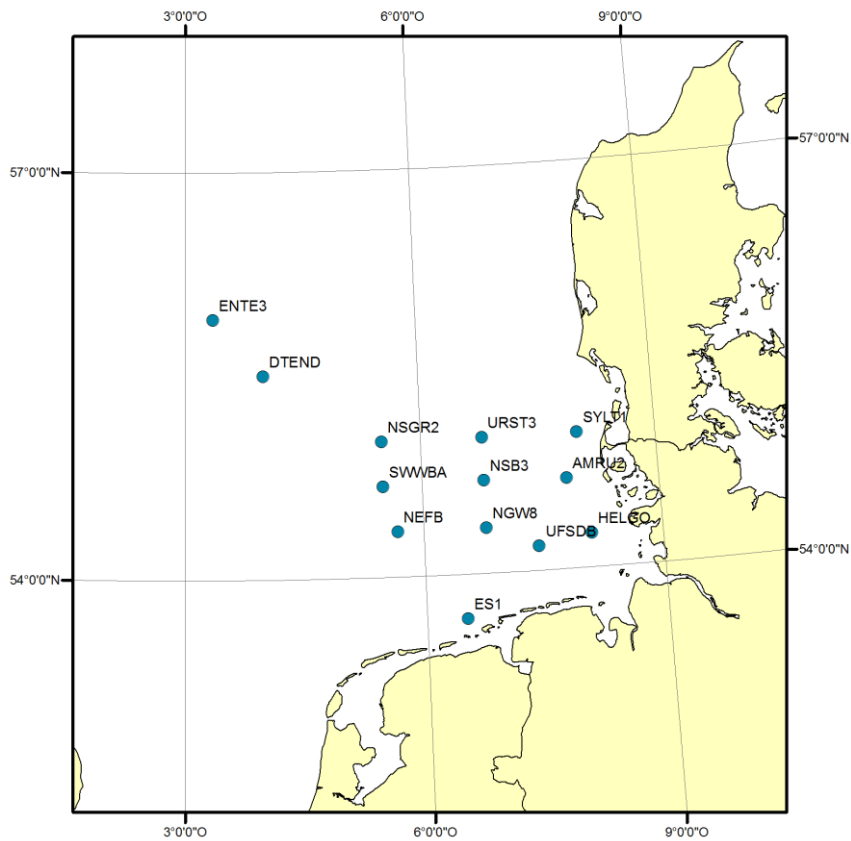


Figure 22: Location of sampling stations with normalized water leaving radiance and chlorophyll-a used for algorithm training (A) and validation (B) of COASTCOLOUR and MERIS products

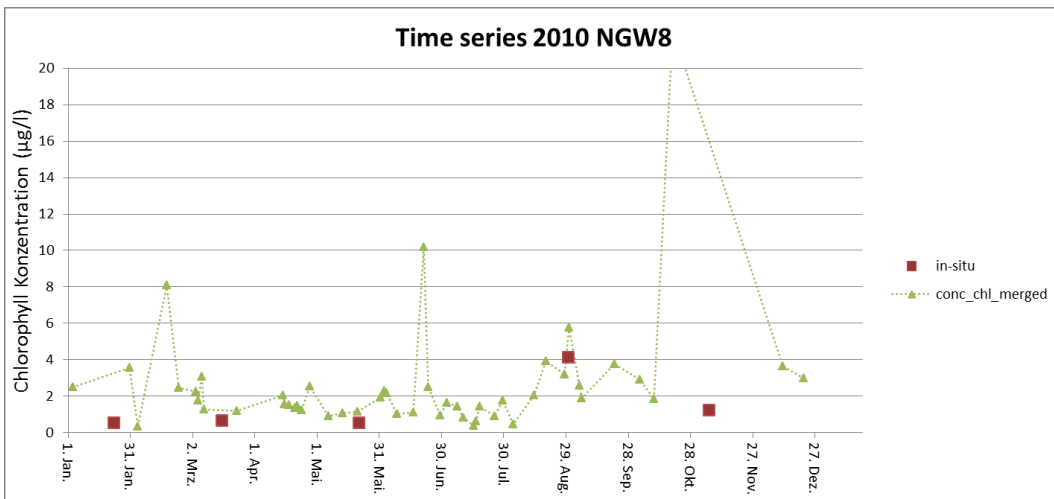
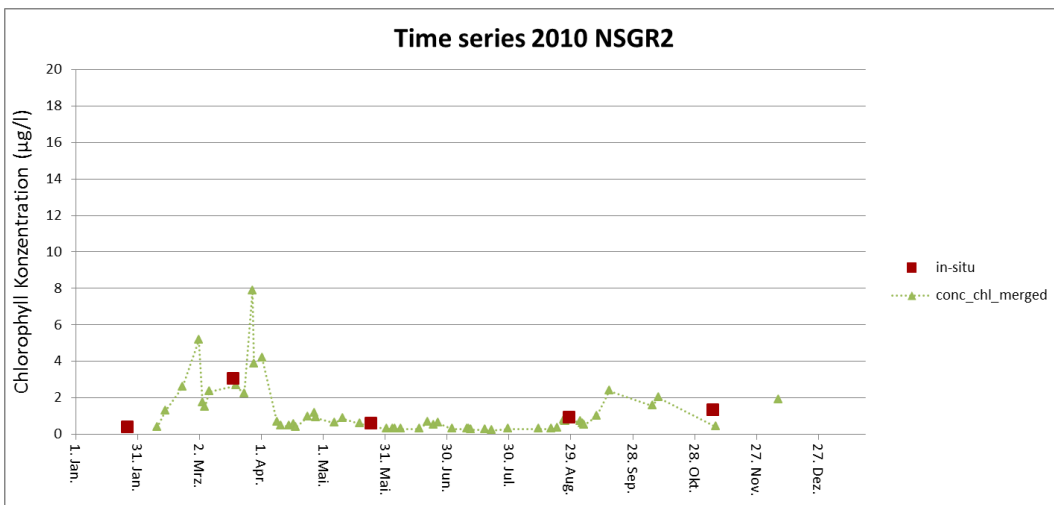
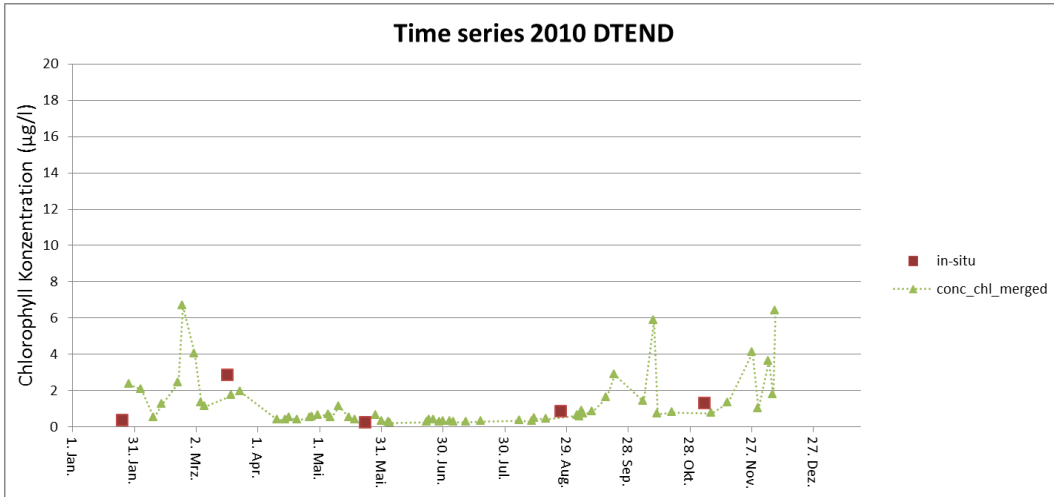
#### 5.4.2 North Sea time series

Time series have been extracted for 2010 for 12 different measurement stations within the North Sea, which have been sampled on 5 days during each year. The stations range from clear water stations to high turbid stations near the coast. A map shows their positions in Figure 23.



**Figure 23: Position of the measurement stations in the North Sea (BSH, Germany)**

The extraction of the chlorophyll concentration has been performed from MERIS RR, 1x1 pixel. The time series in Figure 24 show in red the five measurements from in situ and in green the extracted CC Chlorophyll (conc\_chl\_merged).



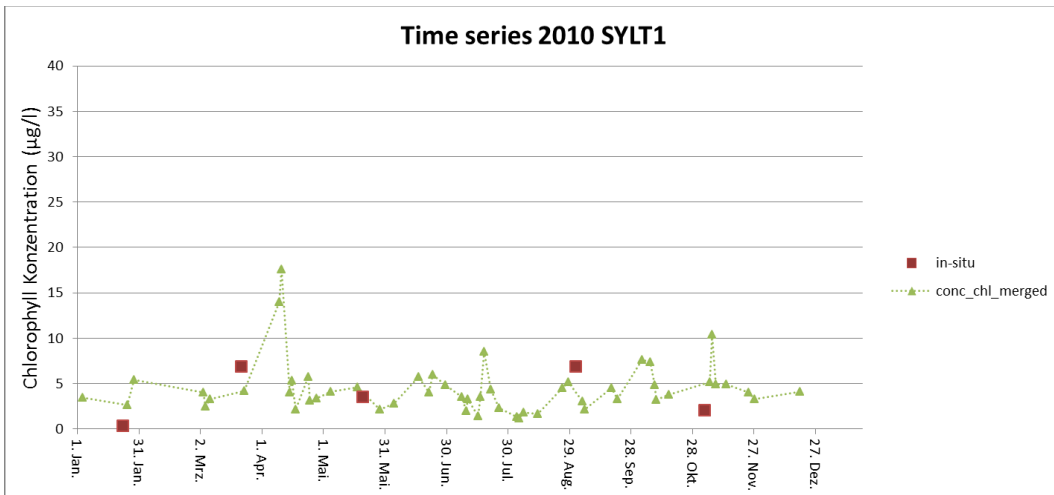
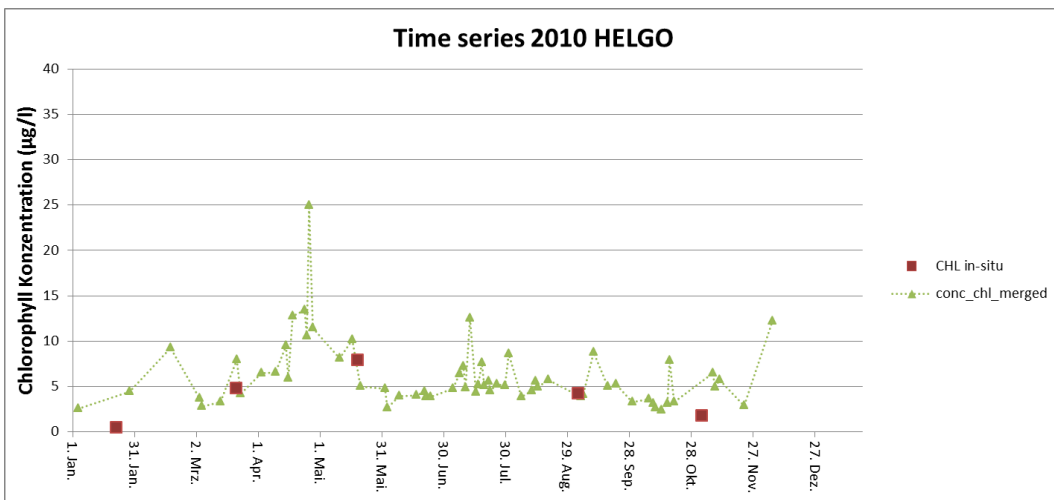
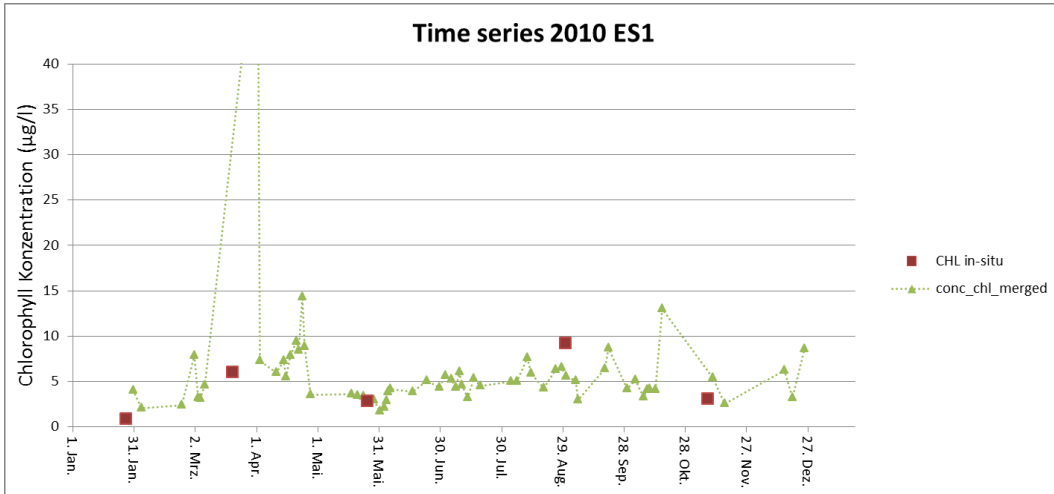


**Figure 24 Time series plots for stations DTEND, NSGR2, NGW8, ES1, HELGO and SYLT1 in the North Sea (2010)**

The plots in Figure 24 are organised from clearer water to more a more turbid water along the eastern parts of the North Sea. The three first plots are scaled until 20 µg/l of chlorophyll concentration, while the three last plots are scaled until 40 µg/l, because the proximity to the coast increases the chances of higher chlorophyll concentration ranges. The adjustment of in situ and observed values is in general quite good. The clear advantage of the satellite data is visible here, with a better

overview of the spring and summer blooms, scarcely noticeable using only in situ data. There are two plots that contained probable outliers in the satellite data: the station NGW8 during October; and the station ES1 in the last days of March. A detail of the satellite water quality parameters for 1 of April 2010, ES1 station, is shown in Figure 25.

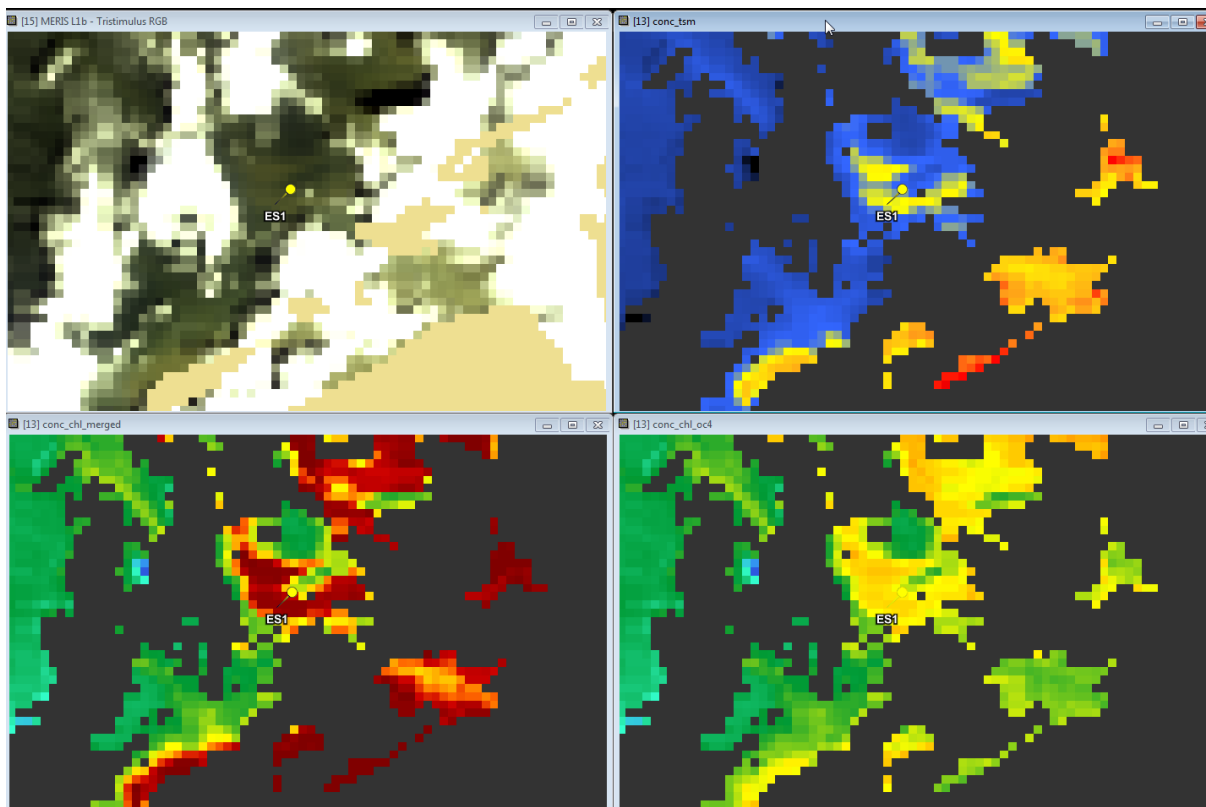
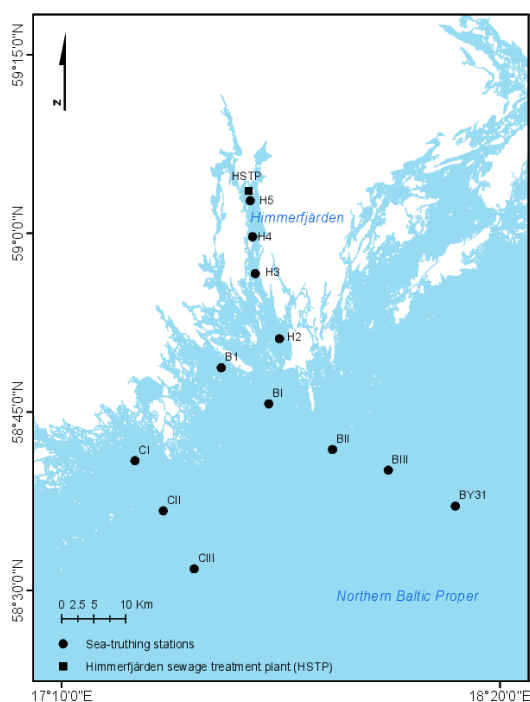


Figure 25 Station ES1, 01.04.2010

### 5.4.3 Baltic Sea (Sweden)

Investigations have been performed on the Swedish Baltic Sea Coast, where different processors have been compared and CoastColour atmospheric correction was related to in situ reflectance measurements. The work summarized here has been performed by José Beltrand during a secondment at Brockmann Consult in the framework of the Peoples project WaterS (Beltrán-Abaunza et al. 2013).

The measurement stations are distributed in the Himmerfjärden and the adjacent coastal areas (Figure 26). Two field campaigns were conducted in July 2008 and spring 2010 (with one additional transect in August 2008). In Himmerfjärden, the chlorophyll a (Chl-a) concentrations that can be observed ranges from  $1 \text{ mg/m}^3$  up to  $18 \text{ mg/m}^3$ , with higher values during the spring bloom. The suspended particulate matter (SPM) load ranges from  $0.5 \text{ g/m}^3$  up to  $2.7 \text{ g/m}^3$ . The absorption of CDOM (g440) in Himmerfjärden ranges from  $0.39 \text{ m}^{-1}$  up to  $1.27 \text{ m}^{-1}$ , and in the open sea from about  $0.3 \text{ m}^{-1}$  to  $0.5 \text{ m}^{-1}$  (Kratzer and Tett, 2009).



**Figure 26: Position of measurement stations in the Baltic Sea and Himmerfjärden**

In situ radiometry was taken with the Tethered Attenuation Coefficient Chain-Sensor (TACCS, manufactured by Satlantic Inc., Canada). The TACCS is an in-water radiometer deployed on a floating buoy. It has an in-water up-welling radiance sensor  $Lu(\lambda)$  with 7 channels matching the MERIS bands centred at 412, 443, 490, 510, 560, 620 and 665 nm. The  $Lu$  radiance sensor has a full-angle field of view (FAFOV) of 20° at nominal depth 0.5 m. MERIS bands centred at 412, 443, 490, 510, 560, 620 and 665 nm. The TACCS includes an in-water chain of  $Ed(\lambda=490\text{ nm})$  at the nominal depths of 2, 4, 6, and 8 m. The TACCS also includes an in-air downward irradiance sensor  $Ed$  centred at 443, 490 and 670 nm. All sensors have a 10 nm bandwidth. TACCS measurements are logged in three minutes intervals at an acquisition rate of 0.5 Hz and approximately at 20 m distance from the ship to avoid ship shading.

The in situ marine reflectance  $p_w$  was calculated accordingly to Kratzer et al. (2008) and Zibordi et al. (2012). This method requires coincident optical profiles taken with the TACCS and using an AC9+ from WET Labs, measuring spectral absorption  $a$  and beam attenuation  $c$  at 412, 440, 488, 510, 532, 555, 630, 676, and 715 nm as described in Kratzer et al. (2008). The marine reflectance was used for the validation of the MERIS reflectance data.

Level 2 datasets consisting of 14 CoastColour-L2R full resolution scenes were used for the study area that coincided with the field measurements of two sea-truthing campaigns. The time difference between in situ measurements and the MERIS overpass was less than two hours for most of the stations investigated here. The CoastColour datasets CCL2R used here were from the CoastColour processing version 1.6.3.

Figure 27 shows the scatterplots and 1:1 lines for the reflectances of the different MERIS bands (412 - 664) and the sea-truthing data using TACCS. The respective error statistical measures are listed in Table 4.

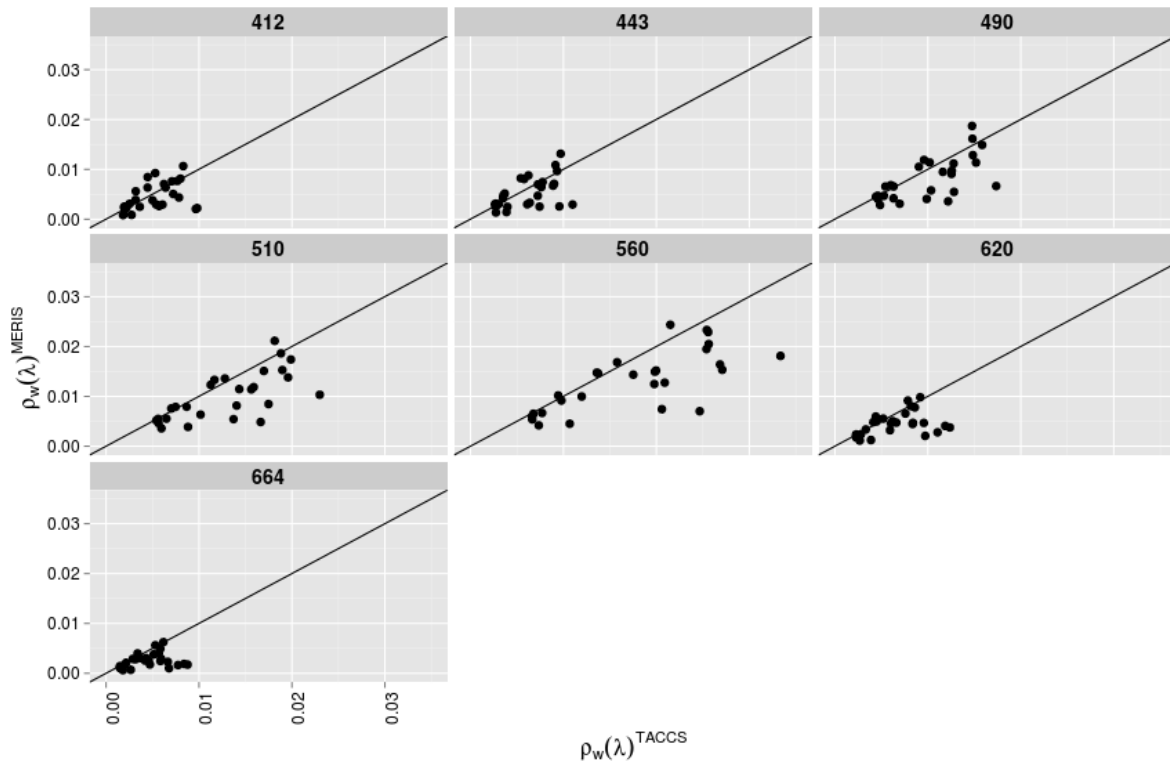


Figure 27: Scatterplots between MERIS reflectance using the CCL2R processor version 1.6.3 and sea-truthing data using TACCS. The number on top of each plot refers to the wavelength expressed in nanometers [nm].

Table 4: Summary of error analysis for MERIS reflectance using the processor CCL2R (N = 27) against sea-truthing data using individual best macro-pixels.

band	wavelength[nm]	MNB[%]	RMS_RD[%]
reflec_1	412	-4.62	46.20
reflec_2	443	-9.58	38.83
reflec_3	490	-16.31	28.74
reflec_4	510	-20.22	24.66
reflec_5	560	-21.96	22.90
reflec_6	620	-23.61	32.38
reflec_7	664	-35.16	30.73

In the framework of this investigation, also other algorithms were tested and compared to each other. The main results concerning the CC AC was that CC L2R datasets showed an increased negative Bias from the blue towards the red bands. Similar tendencies occurred for other processings. The dispersion of the relative differences (RMSRD) for the CoastColour L2R datasets were all below 50%. The CoastColour L2R datasets retrieved a higher number of valid observations compared to other processings.

	Doc:	DEL-27 Validation Report		
	Date:	06.05.2014		
	Issue:	1	Revision:	0

## 6 CONCLUSION

The CoastColour products V2 were successfully validated. The suite of products comprises:

- The Level 1P product, which is a refined top of atmosphere radiance product compared with the standard Level 1b product. It provides improved geolocation, equalisation to reduce coherent noise, smile correction, pixel characterization information (cloud, snow, etc.), a precise coastline and a reformatting into NetCDF following Climate Forecast (CF) conventions.
- The Level L2R product, which is the result of the atmospheric correction. It contains water leaving reflectance, normalised water leaving reflectance and different information about atmospheric properties. It also contains an ortho-corrected geo-coding and different flags characterizing pixels.
- The L2W product, which provides information about water properties such as IOPs, concentrations and other variables. It also contains an ortho-corrected geo-coding and different flags characterizing pixels.

The land-water separation and the cloud screening are the most important pixel classification information available in the Level 1P product. They have been validated by visual comparison with the radiometry (land-water mask) and by quantitative assessment using manually classified pixels. With the latter method producer's accuracy ("probability of detection") of 99% of the cloud masking was established. The producer's accuracy of clear water pixels was 84%. This is an excellent result for a conservative cloud screening, meaning that Level 3 product are basically free of clouds. However, for single products are less stringent cloud screening might be wishes because 15% of the water pixels are lost.

The atmospheric correction of CoastColour has been validated with an excellent performance (RMSE of 0.13,  $R^2=0.90$ ) for all MERMAID match-ups. The investigation of single MERMAID sites showed some differences. While the Atmospheric Correction performs above this global average for the Case1/Case2 site AAOT, its performance decreases for the more turbid site Plumes and Bloomes. However, the case study of the extremely turbid Rio de la Plata has demonstrated that the CC AC works even under extremely high reflective water bodies. The performance for absorbing waters is good compared to other ACs but performs under average compared with the global MERMAID average.

The L2W products were validated against the CoastColour in-situ database, the MERMAID database and were assessed in Case Studies in the North Sea and the Baltic Sea. The CC-insitu and MERMAID investigation provide the global overview, with an overall acceptable result. However, knowing the large variety of optical properties among global coastal sites this is already a big progress. The comparison of the CC chlorophyll with the in-situ chlorophyll reveals also the (known) differences in determination of chlorophyll by in-situ methods. Using the HPLC method, the best correlations are found in site 4 (Morocco), site 26 (Gulf of Mexico) and site 1 (North Sea). The coefficient of determination for TSM seems to be lower than the chlorophyll values, but the correlation is clearly visible. Yellow substance in-situ measurements are very scarce. With only 15 matchups, all in site 3 (Mediterranean and Black Sea), it is not possible to derive firm conclusions. Concerning the Mermaid dataset the regressions show in general good coefficients of correlation for the chlorophyll measurements with fluorometric procedures and HPLC. The best coefficient of determination is found in the comparison of the CC chlorophyll concentration and the fluorometric measures, but the error is lower for the HPLC method that comprises the total chlorophyll\_a from HPLC pigment analysis. The TSM comparison gives good correlation with the in situ data, although only very few match-ups are available in the MERMAID database.

The Case studies for the North Sea, including additional match-ups, transects and time series proved the very good quality of the L2R product. The work performed by PML recommends for the V1 dataset switching to the OC-x algorithm, and validated already L2R + OC3, which is equal to V2 (with OC4 instead of OC3). The transects and time series demonstrate well the good performance of the V2 chlorophyll in comparison with the in-situ data. The Case Study for the Baltic Sea concentrates on the L2R product which was validated with less good results as found in the MERMAID comparison.

	Doc:	DEL-27 Validation Report		
	Date:	06.05.2014		
	Issue:	1	Revision:	0

## 7 REFERENCES

Beltrán-Abaunza, J.M., Kratzer, S.; and Brockmann, C. (2013): Evaluation of MERIS products from Baltic Sea coastal waters rich in CDOM. *Ocean Sci. Discuss.*, 10, 2157-2206

S. Kratzer, C. Brockmann, and G. Moore (2007). Using MERIS full resolution data to monitor coastal waters-A case study from Himmerfjärden, a fjord-like bay in the northwestern Baltic Sea. *Remote Sensing of Environment*, 112:2284 - 2300, 2008. doi:10.1016/j.rse.2007.10.006.

S. Kratzer and P. Tett (2009). Using bio-optics to investigate the extent of coastal waters: A Swedish case study. *Hydrobiologia*, 629:169-186, ISSN 0018-8158. doi:10.1007/s10750-009- 9769-x.

G. Zibordi, K. Ruddick, I. Ansko, G. Moore, S. Kratzer, J. Icely, and A. Reinart (2012). In situ determination of the remote sensing reflectance: an inter-comparison. *Ocean Science Discussions*, 9(2): 787-833, 2012. doi:10.5194/osd-9-787-2012.

## 8 ACKNOWLEDGEMENTS

We acknowledge ACRI-ST, ARGANS and ESA for access to the MERMAID system. (<http://hermes.acri.fr/mermaid>), as well as each one of the PIs contributing with valuable data to the Mermaid database: G. Zibordi, J.Icely, J.F. Berthon, E. Canuti, D. Antoine, D. McKee, H. Klein, G. Mitchell, M. Kahru, S.B. Mustapha, S. Belanger, M. Ondrusek, G. Schuster, B. Holben, H. Loisel, R. Doerffer, A. Gilerson, S. Ahmed, V. bando, C. Belin, K. Voss, K.Hughes, K. Ruddick, H. Sosik, H. Feng, N. Nelson, A. Subramaniam, L.Harding, A.Mannino, R. Gould, R. Arnone, S.Hooker, W.Balch, R. Morrison, K.Carder, F. Muller-Karger, J. Werdell, D. Stramski, D. Siegel, G. Mitchell, Z. Lee, S. Kratzer, G. Tilstone, V. Brotas, P.Y. Deschamps, A. Hommersom, A. Weidemann, B. Gibson.

We acknowledge Jose Beltran to contribute to this report by his work performed within his investigations.

## 9 Annex 1: Validation Report for COASTCOLOUR MERIS Level2 products in Case 2 Waters of the North Sea and Western English Channel

(pdf attached)

European Space Agency contract COASTCOLOUR: Remote Sensing algorithms for coastal waters.

# **Validation Report for COASTCOLOUR MERIS Level2 products in Case 2 Waters of the North Sea and Western English Channel.**

Contract No: ESA - 22807/09/I-AM

**Gavin Tilstone, April 2014.**

Plymouth Marine Laboratory (PML), UK.

## **Executive Summary:**

New MERIS derived Level 2 Reflectance (R) and Water (W) products are available through recent re-processing missions and European Space Agency project COASTCOLOUR. The objective of this report is to validate new MERIS derived Level 2 products to define the most accurate Ocean Colour (OC) chlorophyll-a (Chla) algorithm(s) for the INTERREG-2Seas areas of the North Sea and Western English Channel coastal areas. The report uses full resolution (FR) COASTCOLOUR data with standard Chla (Algal Pigment 2 – AP2) and non-standard (OC3) algorithms to evaluate their potential use in the INTERREG-2Seas area. Using FR COASTCOLOUR Level2R, OC3 proved to be more accurate than AP2 in North Sea and Western English Channel coastal waters.

## 1. Introduction.

Information on marine environmental parameters, such as Chlorophyll a (Chla), is becoming increasingly important as it describes key parameters for monitoring climate change, water quality and the effects of pollution in the marine environment [Justic *et al.*, 1996; Yunev *et al.*, 2005]. Large scale spatial and temporal information on these parameters can be obtained by means of satellite remote sensing, which can aid our understanding of biogeochemical cycles [Bousquet *et al.*, 2006; Mohr and Forsberg, 2002].

Monitoring of water quality in coastal waters is an integral part of water resource management. It allows tracking the effects of anthropogenic influences on the coastal marine environment. In 1988 the European Union adopted new strategy for the Urban Waste Water Treatment Directive and the Nitrates Directive, which resulted in improved legislation on water and bathing water quality. On 23 October 2000, the European Parliament and the Council adopted the Water Framework Directive establishing a framework for Community action in the field of water policy. The water framework directive includes the Bathing Water Directive which aims at achieving 'good ecological status' for all waters and for so-called 'protected areas' such as bathing waters. It resulted in a general definition of ecological quality status for coastal waters based on 19 key parameters which include microbiological, physico-chemical and 'other' parameters. Following this legislation much progress has been made in water protection in Europe and in individual Member States, and also in tackling significant problems at the European level. However Europe's waters are still in need of increased efforts to get them clean or to keep them clean.

To aid monitoring water quality, a range of satellite ocean products have been developed, which has proven successful in areas where the principal optically active material in the water column is phytoplankton. It is however, more difficult to accurately determine Chla from satellite in coastal regions due to their optical complexity [IOCCG, 2000]. Despite their relatively small area, accounting for just 7% of the world ocean's surface, coastal zones play an important part in the global carbon cycle and in buffering human impacts on marine systems. They support 10-15% of the world ocean net annual productivity and may be responsible for > 40 % of the annual carbon sequestration (Muller-Karger *et al.* 2005). Coastal areas of the North Sea are commercially important for fishing and tourism, yet are subject to the increasingly adverse effects of harmful algal blooms [Aanesen *et al.*, 1998; Maestrini and Graneli, 1991], eutrophication [Lancelot *et al.*, 1987] and climate change [Reid *et al.*, 2001; Stige *et al.*, 2006]. There is therefore an obvious need to develop accurate Chla algorithms in coastal regions to monitor these environmental changes. In these regions, where the presence of Coloured Dissolved Organic Material (CDOM) and Total Suspended Material (TSM) also modify the light field [IOCCG, 2000], accurate estimation of Chla from satellite is more difficult. CDOM and TSM originating from riverine run-off and re-suspension of bottom sediment, are highly variable and on a global basis, the combined absorption of coloured dissolved organic and detrital material ( $a_{dg}$ ) contribute up to 40% of the non-water absorption at 440nm in the subtropical gyres and 60% at high latitudes [Siegel *et al.*, 2005].

To facilitate algorithm development, Morel and Prieur [1977] classified optical water types using a simple bipartite segregation into waters where the optical properties

are governed by phytoplankton (Case 1) and those which are additionally affected by  $a_{CDOM}$  and TSM (Case 2) that do not co-vary with phytoplankton. A plethora of algorithms have been developed to detect Chla in Case 1 waters and the most successful was an empirical, band switching ratio which is accurate to 25% for Chla concentrations up to  $3 \text{ mgm}^{-3}$  and was adopted by NASA as the standard SeaWiFS open ocean algorithm [O'Reilly *et al.*, 1998]. This algorithm often fails in Case 2 waters because the optical impact of  $a_{CDOM}$  or TSM can mask phytoplankton absorption at 442nm [Sathyendranath *et al.*, 2001]. As a consequence, Chl estimation is affected by large uncertainties. For example, [Darecki and Stramski, 2004] applied the MODIS case-1 water ocean colour algorithm [Carder *et al.*, 1999] to estimate Chl in the Baltic Sea and obtained a large bias (~30%) and a large random uncertainty (>100%), even after a regionalization of the algorithm.

The availability of data from satellite sensors such as MODIS-Aqua and MERIS, which have more spectral bands and a higher spatial resolution than SeaWiFS plus novel atmospheric correction models, has enabled the development of new products for coastal waters. To facilitate the estimation of Chla from ocean colour in coastal waters, Prieur and Sathyendranath [1981] suggested partitioning the oceans into seven optical water types according to their absorption properties. Recently, a large range of algorithms were developed to retrieve inherent optical properties (IOP) and biogeochemical parameters from optically complex Case 2 waters [Carder *et al.*, 1999; Doerffer and Schiller, 2007; Lee *et al.*, 2002; Maritorena *et al.*, 2002]. The current diversity of IOP models exhibit large differences in performance when retrieving total absorption, backscatter or decomposing these into individual optically active components [IOCCG, 2006], primarily due to a lack of IOP data used to train the models [Claustre and Maritorena, 2003; Cota *et al.*, 2003; Sathyendranath *et al.*, 2001]. This is also compounded by the fact that several combinations of IOP can lead to the same reflectance spectrum when using inverse models [Defoin-Platel and Chami, 2007].

Due to its optical complexity, the North Sea has been a site for satellite algorithm development: A Chla atlas of the region was published using NASA-Coastal Zone Color Scanner (CZCS) global algorithm as a qualitative proof of concept [Holligan *et al.*, 1989]. More recently, a neural network algorithm was developed, firstly calibrated on North Sea data and then globally, to give standard global coastal products of Chla, TSM and  $a_{dg}$  from MERIS data [Doerffer and Schiller, 2007]. Directional water leaving radiance is input to the algorithm and it outputs Chla, TSM and  $a_{dg}$  based on the conversion of scattering and absorption coefficients using non linear multiple inversion solutions and regional conversion factors to give concentrations. Regionally tuned algorithms for the North Sea have also been developed to retrieve Chla [Hokedal *et al.*, 2005; Peters *et al.*, 2005] and TSM [van der Woerd and Pasterkamp, 2004] based on either radiative transfer solutions using the numerical model HYDROLIGHT to estimate concentrations of optically active substances from modeled reflectance spectra or regionally tuned spectral shapes and slopes input to empirical solutions.

In this report we validate a range of standard and non-standard MERIS level2R and 2W products for potential use in monitoring eutrophication in the INTERREG-2Seas region of the North Sea and Western English Channel.

## 2. Methods.

### 2.1. Study area characteristics and sampling regime

Remote Sensing Reflectance ( $R_{rs}(\lambda)$ ) and Chlorophyll-a (Chla) were measured at 594 stations between March 2003 and September 2007 in the North Sea, Western English Channel (WEC) and Celtic Sea (Figure 1).

### 2.2. Measurement of normalized water leaving radiance and Remote Sensing Reflectance.

Measurements of normalized water leaving radiance were performed by MUMM using three TriOS-RAMSES hyperspectral spectro-radiometers, two measuring radiance and one measuring downwelling irradiance as in Ruddick et al. [2006]. The instruments were mounted on a steel frame, so that zenith angles of the sea- and sky viewing radiance sensors were  $40^\circ$ . The frame was fixed to the bow of the ship, facing forward to minimize ship shadow and reflection [Hooker and Morel, 2003]. The ship was maneuvered on station to point the radiance sensors at a relative azimuth angle of  $135^\circ$  away from the sun, to reduce sun glint and bidirectional reflectance effects. IVM used a Photo Research 650 hand held spectro-radiometer. Measurements were from 350 to 950 nm every 10 s for 10 min, coincident with global positioning system (GPS) data. The spectro-radiometers were calibrated before and after the cruise consistent with SeaWiFS protocols [Mueller, 2000]. Water-leaving reflectance ( $\rho_w$ ) was calculated from simultaneous above-water measurements of downwelling irradiance,  $E_d^{0+}$ ; total upwelling radiance (i.e., from the water and from the air-sea interface) at a zenith angle of  $40^\circ$ ,  $L_{sea}^{0+}$ ; and sky radiance,  $L_{sky}^{0+}$ , in the direction of the region of sky that reflects into the sea viewing sensor, by:

$$\rho_w(\lambda) = \pi \frac{L_{sea}^{0+}(\lambda) - \rho_{sky} L_{sky}^{0+}(\lambda)}{E_d^{0+}(\lambda)} \quad (1)$$

where  $\rho_{sky}$  is the air-water interface reflection coefficient for radiance which is equal to the Fresnel reflection coefficient in the case of a flat sea surface and is assumed to be 0.02 for clear skies [Ruddick et al., 2006], which was the case for satellite ‘match-ups’. Residual skylight was removed using baseline correction following Mobley [1999].  $nL_w$  was calculated as follows:

$$nL_w(\lambda) = \frac{\rho_w(\lambda)}{\pi} \times f_0(\lambda) \quad (\text{in mW cm}^{-2} \mu\text{m}^{-1} \text{sr}^{-1}) \quad (2)$$

where  $f_0(\lambda)$  is the mean solar flux above the earth’s atmosphere. The remote sensing reflectance  $R_{rs}(\lambda)$  ( $\text{sr}^{-1}$ ) was then calculated from:

$$R_{rs}(\lambda) = \frac{L_w(\lambda)}{E_s(\lambda, 0^+)} \quad (\text{Equation 1}),$$

where  $E_s(\lambda, 0^+)$  is the above surface downwelling spectral irradiance ( $\text{W m}^{-2} \text{nm}^{-1}$ ) and  $L_w(\lambda)$  is the water leaving radiance ( $\text{W m}^{-2} \text{nm}^{-1} \text{sr}^{-1}$ ). Standard ocean optics protocol [Mueller, 2000] was used in the computation of water leaving radiance ( $L_w$ ), normalised water leaving radiance ( $nL_w$ ) and remote sensing reflectance ( $R_{rs}$ ). Surface downwelling irradiance ( $E_s = (\lambda, 0^+)$ ) was calculated from:

$$E_s(\lambda, 0^+) = (1 + \alpha) E_d(\lambda, 0^-) \quad (\text{Equation 2}),$$

where  $\alpha$  is the Fresnel reflection albedo from air + sky ( $\sim 0.043$ ), and  $E_d(\lambda, 0^-)$  is extrapolated from the  $E_d(\lambda, z)$  profile.

### 2.3. Measurement of Chlorophyll-*a*

On all cruises, surface water samples were collected using 10l Niskin bottles. Between 0.25 and 2 L of seawater were filtered onto 25mm, 0.7  $\mu\text{m}$  GF/F filters and phytoplankton pigments were extracted in methanol containing an internal standard apocarotenolate (Sigma-Aldrich Company Ltd.). Chla extraction was either by freezing at  $-30^\circ\text{C}$  or using an ultrasonic probe following the methods outlined in Sørensen et al. [2007]. Pigments were identified using retention time and spectral match using Photo Diode Array [Jeffrey et al., 1997] and Chla concentration was calculated using response factors generated from calibration using a Chla standard (DHI Water and Environment, Denmark).

Chla from Northern French waters was measured by fluorometry using the methods outlined in Welschmeyer et al. (1994).

### 2.4. Satellite data and algorithms.

Full resolution (FR) MERIS-COASTCOLOUR v2013 processing were extracted by Brockman Consult using ???. Level2R products were used to process Level2W Chla products. The functional form of each of the Chla algorithms tested is given in Table 2 and described in brief, below:

The standard Case 2 MERIS products from the neural network (NN) algorithm [Doerffer and Schiller, 2007] Chla algal pigment 2 (AP2),  $a_{dg}(442)$  and TSM, were extracted using Beam v4.8. The following MERIS quality flags were used to eliminate erroneous data: cloud flag over ocean (CLOUD), land (LAND), no glint correction applied – accuracy uncertain (HIGH\_GLINT), reflectance corrected for medium glint – accuracy maybe degraded (MEDIUM\_GLINT), highly absorbing aerosols (AODB), low sun angle (LOW\_SUN), low confidence flag for water leaving or surface reflectance (PCD1\_13) and reflectance out of range (PCD\_15). The MERIS L2 products were extracted from a 3 x 3 pixel box, within  $\pm 0.5$  hrs of MERIS overpasses.

OC3M is a fourth-order band ratio algorithm, that uses one of two  $R_{rs}(\lambda)/R_{rs}(547)$  ratios (Table 2), depending on the reflectance characteristics of the water type [O'Reilly et al., 2000].

### 2.5. Algorithm Performance.

Initially 594 data points were used from a combination of MERMAID, the Plymouth Marine Laboratory Western English Channel Observatory and IFREMER data bases (Table 1). Of these 594 data, 249 were flagged as ‘suspect L2R flag’, 195 had the ‘invalid L2R flag’ raised and 135 were ‘suspect +invalid L2R flag’, so were eliminated, which resulted in 345 data points for potential match-up analysis. Details of these in situ measurements are given in Table 1 and the location of the points is given in Figure 1A. Of these data, 47 points were  $>1$  hr from MERIS overpass and based on NASA and ESA measurement protocols for satellite validation were therefore used for algorithm validation. The remaining 298 data were used for algorithm calibration.

To evaluate algorithm performance we used the in situ measurements of  $nL_w$  to calculate Chla concentrations. The mean (M), standard deviation (S), and  $\log_{10}$ -root-mean

square ( $\log_{10}$  RMS) of the difference error ( $r$ ) between measured Chla and  $nL_w$  derived Chla at each station were used to evaluate the accuracy of each algorithm as described in Campbell et al. [2002]. The geometric mean and one-sigma range of the inverse transformed ratio between satellite and measured values are given by M ( $F_{med}$ ), M-S ( $F_{min}$ ), M+S ( $F_{max}$ ) and were used as algorithm performance indices. The unbiased percentage difference (UPD) was calculated following Antoine et al. [2008] to illustrate the uncertainty between measured and satellite Chla. We employed one way analysis of variance (ANOVA) to test for significant differences between *in situ* and satellite estimates of Chla. The ANOVA results are given as  $F_{1,823} = x$  and  $P = y$  where F is the mean square to mean square error ratio, the sub-script numbers (1,160) denote the degrees of freedom and P is the ANOVA critical significance value.

Dataset	PI	Location	Lat/Lon	In-situ parameters available	Number of matchup (MEGS 8.0)
Bristol Channel and Irish Sea	David McKee	Bristol Channel & Irish Sea	51/54N -3/-4E	pwN ( $\lambda$ ),pwN_ISME ( $\lambda$ )*,Es ( $\lambda$ ),Chl,IOP,OSM,MSM	43
<a href="#">BSHSummerSurvey</a>	Holger Klein	North sea English Channel	49.0/62.5N -6.0/8.25E	Chl	140
EastEngChannel	Hubert Loisel	Estern English channel	49.4/51.4N 0.0/3.0E	pwN ( $\lambda$ ),Chl	54
<a href="#">Helgoland</a>	Roland Doerffer	North Sea	54N 7.5/8.5E	pwN ( $\lambda$ ),pwN_ISME ( $\lambda$ )*,Es ( $\lambda$ )	N/A
<a href="#">MUMMtriOS</a>	Kevin Ruddick	European Waters	27.35N/53.83N -11.98E/12.50E	pwN ( $\lambda$ ),pwN_ISME ( $\lambda$ )*,Es ( $\lambda$ ),Chl	433
<a href="#">PMLNorthSeaWEC</a>	Gavin Tilstone	North sea Western English Channel	47/53N -10/3.4E	Chl,IOP,TSM	56
<a href="#">REPHY</a>	Catherine Belin	French Coast	41.53/51.10N 9.79/5.10W	Chl,TSM	1284
Wadden Sea	Annelies Hommersom	Wadden Sea	52-53N 4-6W	pwN ( $\lambda$ ),Chl,IOP,TSM	5

**Table 1.** *In situ* data initially used for satellite validation in the INTERREG-2Seas region. Helgoland data were not used, but have been subsequently requested.

### 3. Results

#### 3.1. Accuracy assessment of MERIS COASTCOLOUR Level2R and 2W products in the INTERREG-2Seas Region.

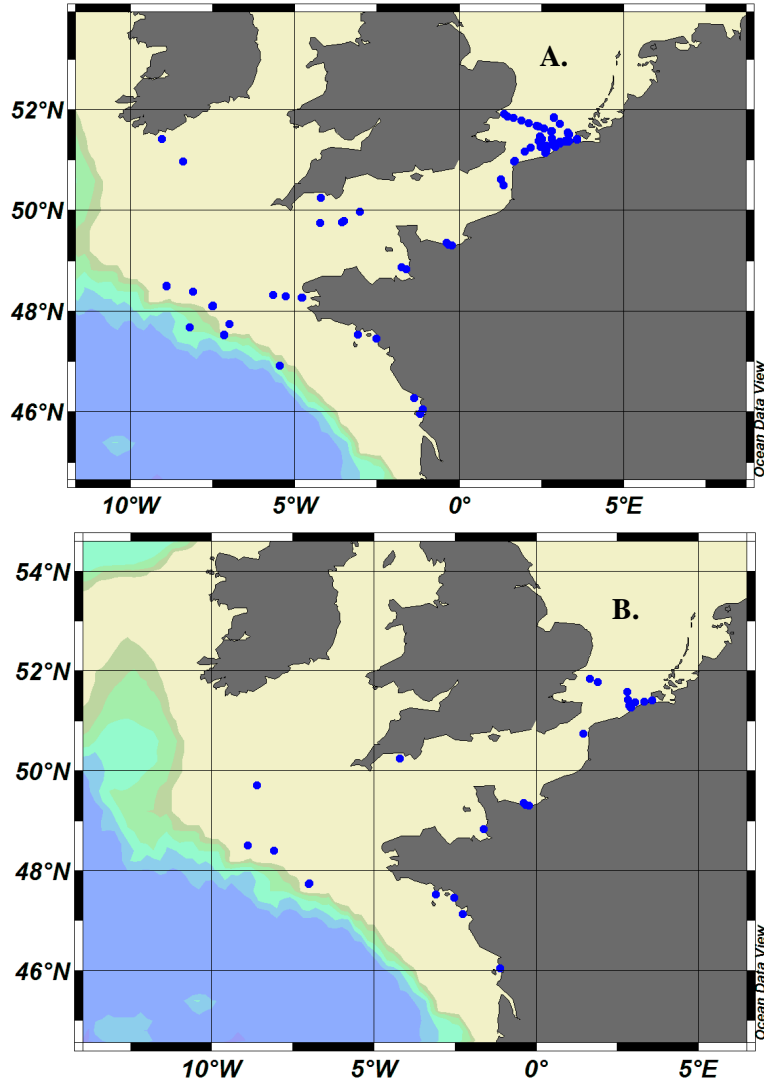


**Figure 1.** Location of sampling stations with normalized water leaving radiance and chlorophyll-a used for algorithm training (A) and validation (B) of COASTCOLOUR and MERIS products.

Firstly we assessed FR COASTCOLOUR Level2R against *in situ*  $R_{rs}$  to evaluate the accuracy of these data as input to the Level2W products (Figure 2). Generally the RMS and bias decreased from  $R_{rs}(412)$  to  $R_{rs}(560)$  and the percentage variation explained also increased from blue to the green wavebands (Table 2) as one would expect due to a higher  $R_{rs}(560)$  signal than  $R_{rs}(412)$ . The range in COASTCOLOUR  $R_{rs}(412)$  at the validation stations was 0.009 to 0.04  $sr^{-1}$ , whereas COASTCOLOUR  $R_{rs}(560)$  was 0.009 to 0.1  $sr^{-1}$ . The statistics listed in Table 2 indicate that COASTCOLOUR Level2R is more accurate in the INTERREG-2Seas area at 560nm than at 412, 443 and 490nm. The RMS and bias increased for  $R_{rs}(665)$ , but so too did the percentage variation explained (Table 2). The regression slope was closer to 1 for COASTCOLOUR from  $R_{rs}(490)$  to  $R_{rs}(665)$  compared to  $R_{rs}(412)$  and  $R_{rs}(442)$  (Figure 2), indicating possible errors in the atmospheric correction at these wave bands.

	412	443	490	510	560	665nm
<b>FR - COASTCOLOUR</b>	<b>N=13</b>					
$R^2$	0.53	0.72	0.83	0.83	0.80	0.89
Slope						
Log <sub>10</sub> - RMS	0.45	0.36	0.26	0.25	0.25	0.45
Bias (S)	0.17	0.14	0.08	0.04	0.05	0.20

**Table 2.** Performance indices for relative errors between *in situ* and COASTCOLOUR at visible wavebands. Percentage variance explained ( $R^2$ ), intercept and slope and log-difference errors in measured and satellite Chla ratio as Mean ( $M$ ), Standard deviation ( $S$ ) and root-mean square (Log<sub>10</sub>-RMS).

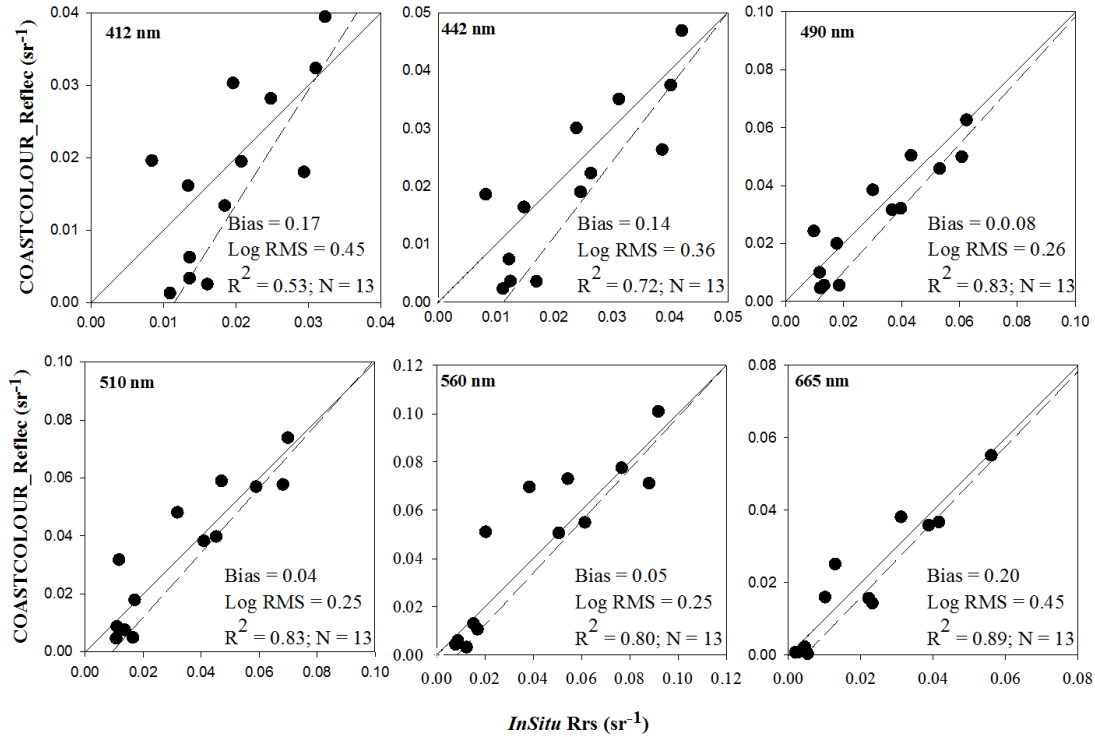


**Figure 2.** Scatter plots of *in situ*  $R_{rs}(\lambda)$  against COASTCOLOUR  $R_{rs}(\lambda)$  for 412, 442, (C) 490, 510, 560 and 665 nm. Faint dotted lines are the 1:1 line, upper and lower 20% quartiles. Solid line is the regression line.

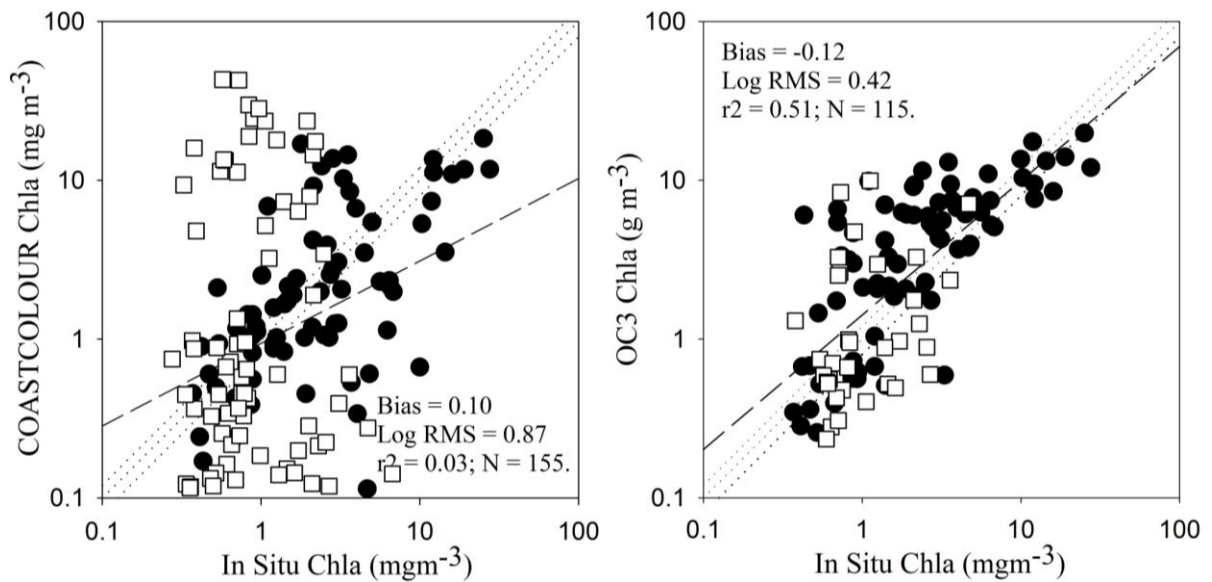


**Figure 3.** Comparison of *in situ* Chla and COASTCOLOUR level2R derived Chla for (A) AP2, (B) OC3 with match-up time of  $\pm 3$  hrs. Faint dotted lines are the 1:1 line, upper and lower 20% quartiles. Solid line is the regression line. Filled circles are data from the North Sea, open squares are from the Western English Channel.

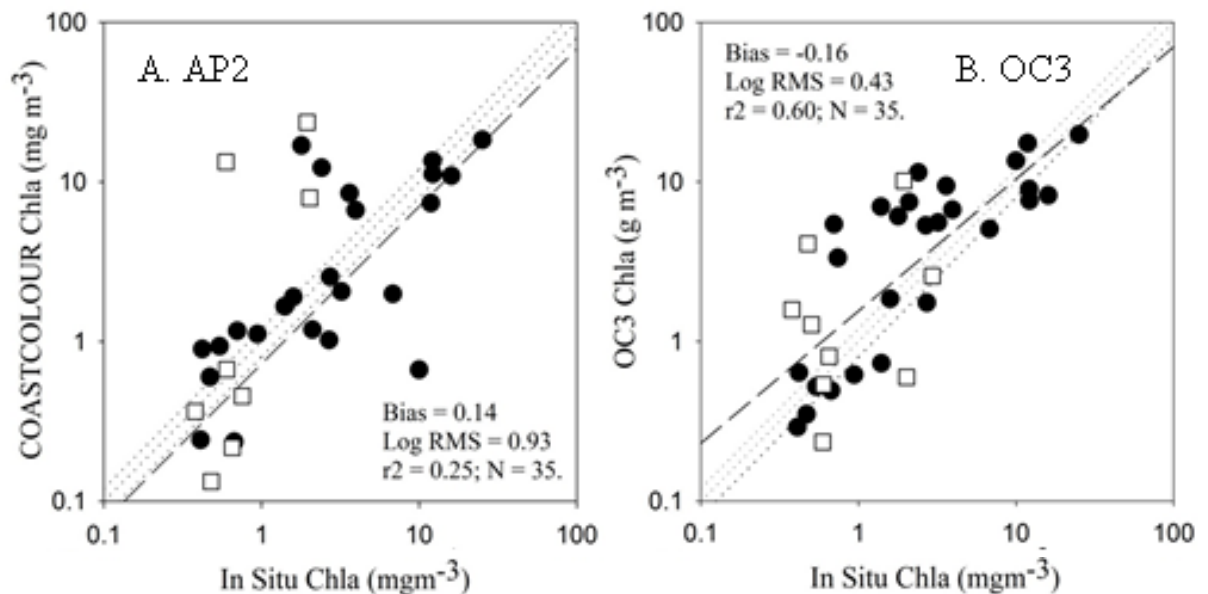


**Figure 4.** Comparison of *in situ* Chla and COASTCOLOUR level2R derived Chla for (A) AP2, (B) OC3 with match-up time  $\pm 45$  mins. Faint dotted lines are the 1:1 line, upper and lower 20% quartiles. Solid line is the regression line. Filled circles are data from the North Sea, open squares are from the Western English Channel.

Comparing COASTCOLOUR Level2W AP2 Chla and OC3 calculated from the COASTCOLOUR Level2R, using a match-up criteria of both  $\pm 3$  hrs (Figure 3) and  $\pm 45$  mins (Figure 4), OC3 had the lowest  $\log_{10}$ -RMS, M, S and intercept and r,  $r^2$ ,  $F_{\text{med}}$  and  $F_{\text{min}}$  closest to 1 and proved to be more accurate than AP2 and across all statistical tests employed (Table 3, Figure 3, 4).

	$R^2$	Slope	Intercept	r	APD	$\text{Log}_{10}$ -RMS	M	S	$F_{\text{med}}$	$F_{\text{max}}$	$F_{\text{min}}$	RMS-E
<b>COAST COLOUR</b>	<b>N=35</b>											
<b>AP2</b>	0.25	0.57	2.78	1.16	<b>77</b>	0.93	0.41	1.04	1.39	11.21	<b>0.17</b>	6.25
<b>OC3</b>	<b>0.58</b>	<b>0.69</b>	<b>2.43</b>	<b>1.15</b>	<b>66</b>	<b>0.43</b>	<b>-0.15</b>	<b>0.39</b>	<b>0.71</b>	<b>1.74</b>	<b>0.29</b>	<b>3.95</b>

**Table 3.** Performance indices for relative errors between *in situ* and  $R_{rs}(\lambda)$  derived Chla for AP2, OC3 (match-up time  $\pm 45$  mins). Percentage variance explained ( $R^2$ ), intercept and slope and log-difference errors in measured and satellite Chla ratio (r) as Mean (M), Standard deviation (S) and root-mean square ( $\text{Log}_{10}$ -RMS). The geometric mean and one-sigma range of the ratio ( $F = \text{Value}_{\text{alg}}/\text{Value}_{\text{meas}}$ ) are given by  $F_{\text{med}}$ ,  $F_{\text{min}}$ , and  $F_{\text{max}}$ , respectively; values closer to 1 are more accurate. UPD is the unbiased percentage difference. The algorithm with the highest Chla precision is highlighted in bold.

#### 4. Discussion.

The objective of this study was to assess the performance of a range Chla algorithms for use the INTERREG-2Seas area of the English Channel and Southern North Sea, that are or have been used as the standard or default algorithm(s) in a range of ocean colour sensors such as SeaWiFS, MODIS and MERIS. *In situ*  $R_{rs}(\lambda)$  and Chla were used to assess the accuracy of three Chla algorithms for monitoring phytoplankton Chla as a proxy for eutrophication in North Sea and Western English Channel coastal waters.

We firstly assessed the accuracy of COASTCOLOUR  $R_{rs}$ . Recent studies based on continuous *in situ* measurements from towers or buoys have shown that MERIS overestimates  $nL_w(442)$  globally, by 44% [Maritorena *et al.*, 2010] and at coastal sites in the Adriatic-Baltic by 39% [Zibordi *et al.*, 2006b; Zibordi *et al.*, 2009], in the Mediterranean by 36% [Antoine *et al.*, 2008] and in the Skagerrak 40% [Sorensen *et al.*, 2007]. In North Sea coastal waters, we found the difference to be 64%. This may be attributed to errors in the standard aerosol model of optical thickness used in the atmospheric correction [Aznavy and Santer, 2009] or to failure in the correction in turbid waters or at cloud borders [Gomez-Chova *et al.*, 2007]. We found that COASTCOLOUR were within 25 % of *in situ* values at blue-green wavebands. At least 65% of the stations in our validation data

set had TSM  $>3.0 \text{ g m}^{-3}$ , where atmospheric correction may start to fail [Esaias *et al.*, 1998], which was evident for MERIS nL<sub>w</sub>(412), nL<sub>w</sub>(442) and nL<sub>w</sub>(490) (Figure 8, Table 2). The difference between *in situ* and MERIS nL<sub>w</sub> improved at 560nm and the 665 nm (Table 2) and the RPD and APD for North Sea coastal areas were similar to those reported both globally (APD; 20% at 560 nm, 125% at 665 nm), in the Baltic and Adriatic (APD; 18% at 560 nm, 47% at 665 nm), the Mediterranean (RPD; 25% at 560 nm, 70% at 665 nm) and in the Skagerrak (RPD; 10% at 560 nm, 40% at 665 nm) [Antoine *et al.*, 2008; Zibordi *et al.*, 2006a].

OC3 was more accurate than the standard AP2 Chla algorithm for North Sea and WEC waters.

AP 2 uses a neural network to derive  $a_{ph}$  and  $b_p$  and through empirical bio-optical relationships, IOP are converted to Chla concentrations. A number of recent papers have highlighted the accuracy of AP2 compared to *in situ* Chla (e.g. Antoine *et al.* 2008; Zibordi *et al.* 2006a; Tilstone *et al.* 2012). Tilstone *et al.* (2012) indicated that there is a tendency for MERIS AP2 in coastal waters of the North Sea and Western English Channel to under-estimate Chla in the range  $<1 \text{ mg m}^{-3}$  and to over-estimate Chla at values  $>6 \text{ mg m}^{-3}$ .

OC3M is a fourth-order band ratio algorithm, that uses one of two  $R_{rs}(\lambda)/R_{rs}(560)$  ratios and either  $R_{rs}(442)/R_{rs}(560)$  or  $R_{rs}(490)/R_{rs}(560)$ , depending on the reflectance characteristics of the water type [O'Reilly *et al.*, 2000]. As outlined in the results section (Figures 3 & 4, Table 2), compared to *in situ*  $R_{rs}(\lambda)$ , for COASTCOLOUR  $R_{rs}(\lambda)$ , the blue-green wavebands  $R_{rs}(490)$  and  $R_{rs}(560)$  were more accurate than  $R_{rs}(442)$  and the retrieval accuracy at this band and  $R_{rs}(412)$  were comparatively poor. This indicates possible errors in the atmospheric correction affecting the blue bands for COASTCOLOUR Level2R. Due to the tendency of MERIS to over-estimate  $R_{rs}(442)$  at low values (i.e. when Chla is high), the use of the  $R_{rs}(442):R_{rs}(560)$  ratio would result in a lower than expected ratio and therefore lower Chla values, which was particularly evident in some areas of the North Sea and Western English Channel with Chla values between 5-10  $\text{mg m}^{-3}$  (Figure 4a). Of the 35 satellite-*in situ* Chla match ups obtained, for OC3 83 % of these used the  $R_{rs}(490):R_{rs}(560)$  ratio. Due to greater errors in  $R_{rs}(443)$  compared to  $R_{rs}(490)$  possibly arising from errors in the atmospheric correction, the accuracy of OC3 was lower than OC5. When OC3 is principally driven by the  $R_{rs}(490):R_{rs}(560)$  ratio, it will be less affected by errors due to high  $a_{CDOM}(\lambda)$  absorption in the blue portion of the spectrum (Tilstone *et al.* 2013). Though there are inherent problems with using band ratios in case 2 waters because the optical properties of  $a_{CDOM}$  or TSM can mask phytoplankton absorption at 442nm, previous studies have found that using more accurate atmospheric correction models such as the bright pixel [Moore *et al.*, 1999], in conjunction with band ratios, satellite estimates of Chla can be as accurate as algorithms that have been designed for case 2 waters [Blondeau-Patissier *et al.*, 2004].

## Conclusions:

In this report, an assessment of COASTCOLOUR level 2R and 2W products was conducted to define the most accurate and appropriate algorithm(s) for the INTERREG-2Seas areas of the North Sea and English Channel coastal areas. The assessment resulted in the following conclusions:

1. From a database of 529 sampling points for Chla from cruises in 2003 to 2009, there were N=35 match-ups at <45 mins from MERIS overpass. It is incredibly difficult to get a large number of high quality match-ups for the INTERREG 2-Seas area using conventional ship borne oceanographic sampling techniques.
2. From the few match-ups available, FR COASTCOLOUR MERIS  $R_{rs}$  at 490, 510, 560 and 665 nm were accurate to  $>0.3 \text{ Log}_{10}\text{-RMS}$  indicating that data at these wavebands can be used to produce potentially accurate Level 2W products.  $R_{rs}$  at 412 and 442 nm were less accurate and showed an inherent under-estimate at both low and high range  $R_{rs}$  values.
3. Using FR COASTCOLOUR Level 2R, OC3 Chla was more accurate than the standard AP2 Chla.

### Acknowledgements.

Thanks to Kevin Ruddick at MUMM, Belgium for providing *in situ*  $R_{rs}$  and Chla data. Thanks to Ruth Airs at the Plymouth Marine Laboratory for providing HPLC data for the Western English Channel Observatory.

### References.

- Aanesen, R. T., H. C. Eilertsen, and O. B. Stabell (1998), Light-induced toxic properties of the marine alga *Phaeocystis pouchetii* towards cod larvae, *Aquatic Toxicology*, 40(2-3), 109-121.
- Antoine, D., F. d'Ortenzio, S. B. Hooker, G. Becu, B. Gentili, D. Tailliez, and A. J. Scott (2008), Assessment of uncertainty in the ocean reflectance determined by three satellite ocean color sensors (MERIS, SeaWiFS and MODIS-A) at an offshore site in the Mediterranean Sea (BOUSSOLE project), *Journal of Geophysical Research-Oceans*, 113, C07013, doi:07010.01029/02007JC004472.
- Aznay, O., and R. Santer (2009), MERIS atmospheric correction over coastal waters: validation of the MERIS aerosol models using AERONET, *International Journal of Remote Sensing*, 30(18), 4663-4684.
- Blondeau-Patissier, D., G. H. Tilstone, V. Martinez-Vicente, and G. F. Moore (2004), Comparison of bio-physical marine products from SeaWiFS, MODIS and a bio-optical model with *in situ* measurements from Northern European waters, *Journal of Optics a-Pure and Applied Optics*, 6(9), 875-889.
- Bousquet, P., et al. (2006), Contribution of anthropogenic and natural sources to atmospheric methane variability, *Nature*, 443(7110), 439-443.
- Campbell, J., et al. (2002), Comparison of algorithms for estimating ocean primary production from surface chlorophyll, temperature, and irradiance, *Global Biogeochemical Cycles*, 16(3), art. no.-1035.
- Carder, K. L., F. R. Chen, Z. P. Lee, S. K. Hawes, and D. Kamykowski (1999), Semianalytic Moderate-Resolution Imaging Spectrometer algorithms for chlorophyll a and absorption with bio-optical domains based on nitrate-depletion temperatures, *Journal of Geophysical Research-Oceans*, 104(C3), 5403-5421.
- Claustre, H., and S. Maritorena (2003), The many shades of ocean blue, *Science*, 302(5650), 1514-1515.
- Cota, G. F., W. G. Harrison, T. Platt, S. Sathyendranath, and V. Stuart (2003), Bio-optical properties of the Labrador Sea, *Journal of Geophysical Research-Oceans*, 108(C7), C73228, doi:73210.71029/72000JC000597

Darecki, M., and D. Stramski (2004), An evaluation of MODIS and SeaWiFS bio-optical algorithms in the Baltic Sea, *Remote Sensing of Environment*, 89(3), 326-350.

Defoin-Platel, M., and M. Chami (2007), How ambiguous is the inverse problem of ocean color in coastal waters?, *Journal of Geophysical Research-Oceans*, 112(C3), 1 - 16.

Doerffer, R., and H. Schiller (2007), The MERIS case 2 water algorithm, *International Journal of Remote Sensing*, 28(3-4), 517-535.

Esaias, W. E., et al. (1998), An overview of MODIS capabilities for ocean science observations, *Ieee Transactions on Geoscience and Remote Sensing*, 36(4), 1250-1265.

Gomez-Chova, L., G. Camps-Valls, J. Calpe-Maravilla, L. Guanter, and J. Moreno (2007), Cloud-screening algorithm for ENVISAT/MERIS multispectral images, *Ieee Transactions on Geoscience and Remote Sensing*, 45(12), 4105-4118.

Hokedal, J., E. Aas, and K. Sorensen (2005), Spectral optical and bio-optical relationships in the Oslo Fjord compared with similar results from the Baltic Sea, *International Journal of Remote Sensing*, 26(2), 371-386.

Holligan, P. M., T. Aarup, and S. B. Groom (1989), The North-Sea - Satellite Color Atlas, *Continental Shelf Research*, 9(8), 665-765.

Hooker, S. B., and A. Morel (2003), Platform and environmental effects on above-water determinations of water-leaving radiances, *Journal of Atmospheric and Oceanic Technology*, 20(1), 187-205.

IOCCG (2000), Remote sensing of Ocean Colour in Coastal and Other Optically-Complex Waters. Rep. 3, 1-137 pp, Bedford Institute of Oceanography, Canada.

IOCCG (2006), *Remote Sensing of Inherent Optical Properties: Fundamentals, tests of algorithms and 774 applications*, IOCCG, Dartmouth, Canada.

Jeffrey, S. W., R. F. C. Mantoura, and S. W. Wright (1997), *Phytoplankton pigments in oceanography*, UNESCO, Paris.

Justic, D., N. N. Rabalais, and R. E. Turner (1996), Effects of climate change on hypoxia in coastal waters: A doubled CO<sub>2</sub> scenario for the northern Gulf of Mexico, *Limnology and Oceanography*, 41(5), 992-1003.

Lancelot, C., G. Billen, A. Sournia, T. Weisse, F. Colijn, M. J. W. Veldhuis, A. Davies, and P. Wassman (1987), Phaeocystis Blooms and Nutrient Enrichment in the Continental Coastal Zones of the North-Sea, *Ambio*, 16(1), 38-46.

Lee, Z. P., K. L. Carder, and R. A. Arnone (2002), Deriving inherent optical properties from water color: a multiband quasi-analytical algorithm for optically deep waters, *Applied Optics*, 41(27), 5755-5772.

Maestrini, S. Y., and E. Graneli (1991), Environmental-Conditions and Ecophysiological Mechanisms Which Led to the 1988 Chrysochromulina-Polylepis Bloom - an Hypothesis, *Oceanologica Acta*, 14(4), 397-413.

Maritorea, S., D. A. Siegel, and A. R. Peterson (2002), Optimization of a semianalytical ocean color model for global-scale applications, *Applied Optics*, 41(15), 2705-2714.

Maritorea, S., O. H. F. d'Andon, A. Mangin, and D. A. Siegel (2010), Merged satellite ocean color data products using a bio-optical model: Characteristics, benefits and issues, *Remote Sensing of Environment*, 114(8), 1791-1804.

Mobley, C. D. (1999), Estimation of the remote sensing reflectance from above-surface measurements., *Applied Optics*, 38(36), 7442-7455.

Mohr, J. J., and R. Forsberg (2002), Remote sensing: Searching for new islands in sea ice - Coastlines concealed in polar seas are now more accessible to cartography, *Nature*, 416(6876), 35-35.

Moore, G. F., J. Aiken, and S. J. Lavender (1999), The atmospheric correction of water colour and the quantitative retrieval of suspended particulate matter in Case II waters: application to MERIS, *International Journal of Remote Sensing*, 20(9), 1713-1733.

Morel, A., and L. Prieur (1977), Analysis of variations in ocean color, *Limnology and Oceanography*, 22, 709-722.

Mueller, J. L. e. a. (2000), Above-water radiance and remote sensing reflectance measurements and analysis protocols, in *Ocean optics protocols for satellite ocean color sensor validation.*, edited by G. S. Fargion and J. L. Mueller, National Aeronautical and Space Administration., Washington, USA.

O'Reilly, J. E., S. Maritorena, B. G. Mitchell, D. A. Siegel, K. L. Carder, S. A. Garver, M. Kahru, and C. McClain (1998), Ocean color chlorophyll algorithms for SeaWiFS, *Journal of Geophysical Research-Oceans*, 103(C11), 24937-24953.

O'Reilly, J. E., et al. (2000), Volume 11, SeaWiFS postlaunch calibration and validation analyses, Part 3, *NASA Technical Memorandum - SeaWiFS Postlaunch Technical Report Series(11)*, 1-49.

Peters, S. W. M., et al. (2005), *An atlas of Chlorophyll-a concentrations for the North Sea based on MERIS imagery of 2003.*, Edition 3. ed., Vrije Universiteit, Amsterdam, Amsterdam, The Netherlands.

Prieur, L., and S. Sathyendranath (1981), An Optical Classification of Coastal and Oceanic Waters Based on the Specific Spectral Absorption Curves of Phytoplankton Pigments, Dissolved Organic-Matter, and Other Particulate Materials, *Limnology and Oceanography*, 26(4), 671-689.

Reid, P. C., M. D. Borges, and E. Svendsen (2001), A regime shift in the North Sea circa 1988 linked to changes in the North Sea horse mackerel fishery, *Fisheries Research*, 50(1-2), 163-171.

Ruddick, K. G., V. De Cauwer, Y. J. Park, and G. Moore (2006), Seaborne measurements of near infrared water-leaving reflectance: The similarity spectrum for turbid waters, *Limnology and Oceanography*, 51(2), 1167-1179.

Sathyendranath, S., G. Cota, V. Stuart, H. Maass, and T. Platt (2001), Remote sensing of phytoplankton pigments: a comparison of empirical and theoretical approaches, *International Journal of Remote Sensing*, 22(2-3), 249-273.

Siegel, D. A., S. Maritorena, N. B. Nelson, M. J. Behrenfeld, and C. R. McClain (2005), Colored dissolved organic matter and its influence on the satellite-based characterization of the ocean biosphere, *Geophysical Research Letters*, 32(20), L20605.

Sorensen, K., E. Aas, and J. Hokedal (2007), Validation of MERIS water products and bio-optical relationships in the Skagerrak, *International Journal of Remote Sensing*, 28(3-4), 555-568.

Stige, L. C., G. Ottersen, K. Brander, K. S. Chan, and N. C. Stenseth (2006), Cod and climate: effect of the North Atlantic Oscillation on recruitment in the North Atlantic, *Marine Ecology-Progress Series*, 325, 227-241.

van der Woerd, H., and R. Pasterkamp (2004), Mapping of the North Sea turbid coastal waters using SeaWiFS data, *Canadian Journal of Remote Sensing*, 30(1), 44-53.

Yunev, O. A., S. Moncheva, and J. Carstensen (2005), Long-term variability of vertical chlorophyll a and nitrate profiles in the open Black Sea: eutrophication and climate change, *Marine Ecology-Progress Series*, 294, 95-107.

Zibordi, G., F. Melin, and J. F. Berthon (2006a), Comparison of SeaWiFS, MODIS and MERIS radiometric products at a coastal site, *Geophysical Research Letters*, 33(6).

Zibordi, G., N. Strombeck, F. Melin, and J. F. Berthon (2006b), Tower-based radiometric observations at a coastal site in the Baltic Proper, *Estuarine Coastal and Shelf Science*, 69(3-4), 649-654.

Zibordi, G., J. F. Berthon, F. Melin, D. D'Alimonte, and S. Kaitala (2009), Validation of satellite ocean color primary products at optically complex coastal sites: Northern Adriatic Sea, Northern Baltic Proper and Gulf of Finland, *Remote Sensing of Environment*, 113(12), 2574-2591.